

Development of a system protection model against voltage collapse in PSS/E

Master's thesis in Electrical Power Engineering

David Stenberg
Joakim Åkesson

MASTER'S THESIS IN ELECTRICAL POWER ENGINEERING

Development of a system protection model against voltage collapse in PSS/E

DAVID STENBERG
JOAKIM ÅKESSON



CHALMERS
UNIVERSITY OF TECHNOLOGY

Division of Electric Power Engineering
Department of Energy & Environment
CHALMERS UNIVERSITY OF TECHNOLOGY
Gothenburg 2016

Development of a system protection model against voltage collapse in PSS/E
Master's thesis in Electrical Power Engineering
DAVID STENBERG
JOAKIM ÅKESSON

© DAVID STENBERG
JOAKIM ÅKESSON, 2016.
All rights reserved.

Supervisor and Examiner: Anh Tuan Le, Division of Electric Power Engineering

Division of Electric Power Engineering
Department of Energy & Environment
Chalmers University of Technology
SE-412 96 Gothenburg
Sweden
Telephone +46 (0)31-772 1000

Cover:

Illustrates the TPSI value of the second scenario in the study of the Nordic32,
blue without the system protection model and red with the model implemented.

Typset in L^AT_EX.
Chalmers Reproservice
Gothenburg 2016

Development of a system protection model against voltage collapse in PSS/E

DAVID STENBERG

JOAKIM ÅKESSON

Division of Electric Power Engineering

Department of Energy & Environment

Chalmers University of Technology

Abstract

This thesis investigates voltage instability leading to voltage collapse in PSS/E and how such scenario can be prevented by the use of a system protection model which has been proposed and developed in this thesis. The model sees the system as a whole and can initiate a system protection response based on a voltage stability indicator in parallel with signals from over excitation limiters (OELs).

Three case studies were performed for evaluating two well-known voltage stability indicators in the literature, namely the Impedance Stability Index (ISI) and the Transmission Path Stability Index (TPSI). The two first studies showed that one of two methods to calculate the ISI gave a more stable result, which was selected to be used in later case studies. Both indicators were then used and evaluated in a third case study consisting of the Nordic 32-bus test system developed by Svenska Kraftnät. In this case study, two separate contingency scenarios were designed to cause a voltage collapse. It was found that the calculations of the ISI were time consuming and did not indicate the margin to voltage collapse as clearly as the TPSI did.

The TPSI and signals from OELs were used as input signals in the system protection model designed to protect the power system. The model was designed to generate control signals to change Automated Voltage Regulator (AVR) set-points of synchronous generators and initiate load shedding schemes. The functionality of the system protection model was successfully verified when its implementation in PSS/E was able to prevent the voltage collapse scenarios designed in the third case study. Voltage collapse in the first scenario was prevented by increasing AVR set-points when OELs were activated and the TPSI value was lower than 0.15. The second scenario was more severe and it was necessary to utilize both increasing AVR set-points and as load shedding which was initialized when the TPSI dropped below a threshold of 0.05.

Keywords: Voltage stability, Voltage stability indicators, Impedance stability index (ISI), Transmission path stability index (TPSI), PSS/E, System protection relay model, Automatic voltage regulator (AVR), Load shedding

Acknowledgement

This is a M.Sc thesis at the division of Electrical Power Engineering at the Department of Energy & Environment at Chalmers University of Technology in Gothenburg, Sweden.

First of all we would like to thank our supervisor Anh Tuan Le for all feedback and help throughout the work with this thesis. A special thanks to Mattias Persson who have helped us with creating the user-defined model in PSS/E constituting our system protection model and to Peiyuan Chen for much needed support.

David Stenberg & Joakim Åkesson, Gothenburg, June 15, 2016

Contents

Abstract	vi
Acknowledgments	vii
Contents	ix
List of Figures	xi
List of Tables	xv
Glossary	xx
Abbreviations	xxi
1 Introduction	1
1.1 Problem	2
1.2 Purpose of the thesis	2
1.3 Delimitations	2
1.4 Method	3
1.5 Thesis outline	4
2 Technical Background	5
2.1 Voltage stability	5
2.1.1 PV and VQ curves and system stability	6
2.1.2 The effects of contingencies on voltage stability	7
2.1.3 Reactive power compensation	8
2.1.4 Online load tap changers (OLTC)	9
2.1.5 Over excitation limiters (OEL)	10
2.1.6 Voltage instability and voltage collapse	11

2.1.7	Causes of voltage instability	11
2.2	Previous work on voltage stability indicators	12
2.3	Voltage stability indicators	12
2.3.1	Impedance stability index (ISI)	13
2.3.2	Transmission path stability index (TPSI)	16
2.3.3	S-difference indicator (SDI)	20
2.3.4	Fast Voltage Stability Index (FVSI)	21
2.3.5	Indicator comparison	23
2.3.6	Choice of voltage stability indicators	24
2.4	Preventing voltage collapse	24
2.4.1	Load Shedding	24
2.4.2	Exciter control and increasing AVR set-point	25
2.4.3	FACTS devices	25
2.5	Simulation Models	26
2.5.1	Essential models regarding voltage stability	26
2.5.2	Additional models	27
3	Evaluation of voltage stability indicators	29
3.1	Two-bus case study	29
3.1.1	Network setup	30
3.1.2	Indicator evaluation: Two-bus system, without switched shunt compensation	30
3.1.3	Indicator evaluation: Two-bus system, with switched shunt compensation	32
3.1.4	Discussion	33
3.2	Three-bus case study	33
3.2.1	Network setup	34
3.2.2	Indicator evaluation	35
3.2.3	Discussion	37
3.3	Nordic32 case study	37
3.3.1	Network setup	38
3.3.2	Voltage instability cases	40
3.3.3	Indicators evaluation	44
3.3.4	Discussion	45
4	Prevention of voltage collapse	47
4.1	The implementation of the system protection model	47
4.2	Model working principle	48
4.3	Settings of the model	48
4.4	Verification of the model	49
4.5	Evaluation of the system protection model	50

4.5.1	Case 1	50
4.5.2	Case 2	52
4.6	Discussion	55
5	Conclusions and future work	57
5.1	Conclusions	57
5.2	Future work	58
	References	63
A	Simulation model data	A1
A.1	Two-bus case study	A1
A.1.1	Generator data	A1
A.1.2	Branch data	A1
A.1.3	Load data	A2
A.1.4	Switched shunt data	A2
A.2	Three-bus case study	A2
A.2.1	Generator data	A2
A.2.2	Branch data	A3
A.2.3	Load data	A3
A.3	Nordic32 case studies	A3
A.3.1	Case 1 data	A3
A.3.2	Case 2 data	A4
A.3.3	DISTR1 Mho settings used in the Nordic32	A5
B	System protection relay model data sheet	A1
C	System protection relay model Fortran code	A1

List of Figures

2.1	PV and VQ curves illustrating a system with a constant power factor, with no injected reactive power and with a constant load. (a) Voltage as a function of transferred active power with a constant power factor and with no injected reactive power. (b) Voltage as a function of transferred reactive power with a constant load.	7
2.2	The characteristics of PV and QV curves when one, two or three lines carries the power transfer between two buses. (a) Voltage as a function of transferred active power as the operating point for the voltage decreases with less lines in parallel. (b) Voltage as a function of transferred reactive power as reactive power losses is affected with less lines in parallel.	8
2.3	Reactive power as a function of voltage and the associated shunt compensation as a function of voltage.	9
2.4	π -model of a OLTC with series admittance y_t and tap-ratio a	10
2.5	Equivalent circuit of a two bus network showing the generator reactance X_d which is added in series with X_T and Z_{Thv} when the OEL is active, thus increasing the impedance.	10
2.6	Thévenin equivalent of a simple power system network.	14
2.7	Thévenin equivalent illustrating the thévenin impedance Z'_{Thv} which includes the load impedance.	16
2.8	Voltage drop $V_s - V_r \cos \delta$ between sending end and receiving end projected on the sending end bus voltage phasor V_s	17
2.9	Voltage drops of a transmission path projected on the sending end bus voltage phasor V_1 . Resulting in a sum of voltage drops $\Delta V'_d$. . .	18
2.10	Directed graph with four different possible paths from node one to seven.	19

2.11	Two bus system used to explain FVSI, V_i and V_j are sending and receiving end voltage and I the current flowing in the line with characteristics $R + jX$ between the two load buses.	22
3.1	The 2-bus network used in the simulation for verifying voltage indicators when no shunt compensation is active.	30
3.2	Performance of the voltage stability indicators ISI and TPSI for a two bus system without compensation. (a) Voltage and voltage stability indicators as a function of the active power consumed by the load. (b) Active power consumed by the load and voltage stability indicators as a function of time.	31
3.3	Performance of the voltage stability indicators ISI and TPSI for a two bus system with compensation. (a) Voltage and voltage stability indicators as a function of the active power consumed by the load. (b) Active power consumed by the load and voltage stability indicators as a function of time.	32
3.4	The 3-bus network used in the simulation for verifying the TPSI and ISI.	34
3.5	Performance of the voltage stability indicators ISI and TPSI in the three bus case study. (a) Voltage and ISI indicator at bus 2 as a function of the time. (b) Voltage, ISI and TPSI at bus 3 as a function of the time.	35
3.6	Characteristics of the load impedance and the thévenin impedance at bus 3 as a function of time for the three bus case study.	36
3.7	The Nordic32 network which was used for verifying the implementation of the protection model.	39
3.8	Indicator values and voltage characteristics as a function of time of the first case study in the Nordic32 test system. (a) The characteristics of TPSI and ISI of the weakest bus for the first case study of the Nordic32 test system. (b) The voltage characteristics of the buses 1042, 1043, 4042 and 4047 which are most affected of the first case study of the Nordic32 test system.	42
3.9	Frequency characteristic at bus 1041 which is the weakest bus in Case 1. All buses do however show similar frequency characteristics.	42
3.10	Indicator values and voltage characteristics as a function of time of the second case study in the Nordic32 test system. (a) The characteristics of TPSI and ISI of the weakest bus for the second case study of the Nordic32 test system. (b) The voltage characteristics of the buses 1042, 1043, 4042 and 4047 which are most affected of the second case study of the Nordic32 test system.	43

3.11	Frequency characteristic at bus 4042 where 720 MVA of generation is lost in the beginning of the simulation.	44
4.1	Block diagram of the system protection model which is run at each simulation time step in PSS/E	48
4.2	A comparison between calculating the TPSI with Matlab and with the system protection model as well as the filtered signal of the TPSI. TPSI calculated by both Matlab and the system protection model as well as a filtered TPSI signal for Case 1 in (a) . TPSI calculated by both Matlab and the system protection model as well as a filtered TPSI signal for Case 2 in (b)	49
4.3	Case 1 TPSI in (a) and bus voltages in (b) for critical buses after the fault with corrective actions through AVR set-point increase performed by the system protection model resulting in a prevention of voltage collapse.	50
4.4	Reactive power production in (a) and voltages in (b) for bus 1022 which generator experienced activation of OEL and therefore initiated the AVR set-points increase and for bus 4021 which is one of the buses with increased AVR set-points	52
4.5	Case 2 TPSI in (a) and bus voltages in (b) for critical buses after the fault with corrective actions through AVR set-point increase performed by the system protection model resulting in a prevention of voltage collapse.	53
4.6	Apparent load power in (a) and bus voltages in (b) for bus 42 and 46 which experience load shedding at 53 and 100 seconds respectively.	54

List of Tables

2.1	Table over additional models used for the dynamic simulations of the Nordic32 test system.	28
3.1	Sequence of events leading to voltage collapse in the first case study of the Nordic32 test system.	41
3.2	Sequence of events leading to voltage collapse in the second case study of the Nordic32.	43
4.1	Sequence of events for Case 1 with the system protection model . . .	51
4.2	Sequence of events for Case 2 with the system protection relay model	53
A1	Generator data used in the simulation for the two bus case study, dynamic data from .dyr file.	A1
A2	Branch data used in the simulation for the two bus case study . . .	A1
A3	Load data used in the simulation for the two bus case study, a constant power factor of $\cos \phi=0.95$ was used.	A2
A4	Switched shunt data used in the simulation for the two bus case study	A2
A5	Generator data used for both generators in the simulation for the three bus case study, dynamic data from .dyr file.	A2
A6	Branch data used for all three branches in the simulation for the three bus case study.	A3
A7	Load data used for both loads in the simulation for the three bus case study.	A3
A8	Modified load data used for Case 1 in the Nordic32, remaining buses have original load levels.	A3
A9	Modified load data used for Case 2 in the Nordic32, remaining buses have original load levels.	A4
A10	DISTR1 Mho settings used in the Nordic32, trip times are set to 2.5, 15 and 30 cycles for the three zones respectively.	A6

A1 Model CONs, STATEs, VARs and ICONs A1

Glossary

sign	description	unit
E_t	Generator terminal voltage	[V]
P	Active power	[W]
Q	Reactive power	[VAr]
Q_C	Reactive power compensation	[VAr]
Q_L	Reactive power, load	[VAr]
S	Apparent power	[VA]
X_d	Generator reactance	[Ω]
X_{Sh}	Shunt reactance	[Ω]
Z_{Load}	Load impedance	[Ω]
Z_{Thv}	Thévenin impedance	[Ω]
δ	Voltage angle	[rad]
E	Voltage at sending end	[V]
I_{ij}	Current between bus i and j	[A]
I	Current	[A]
P_r	Apparent power at receiving end	[VA]
P_{Load}	Active power, load	[W]
R	Resistance	[Ω]
S_j	Apparent power at bus j	[VA]
V_i	Voltage at bus i	[V]
V_j	Voltage at bus j	[V]

sign	description	unit
V	Voltage at receiving end	[V]
X_T	Generator transformer impedance	[Ω]
X	Line impedance	[Ω]
y_t	Series admittance of transformer	[S]

Abbreviations

AVR	Automatic Voltage Regulator
FACTS	Flexible Alternating Current Transmission System
FVSI	Fast Voltage Stability Index
GSF	Generation Shift Factor
ISI	Impedance Stability Index
OEL	Overexcitation Limiter
PMU	Phasor Measurement Unit
PSS/E	Power System Simulator for Engineering
SCADA	Supervisory Control And Data Acquisition
SDI	S-Difference Indicator
SPS	System Protection Scheme
SVC	Static Var Compensator
TPSI	Transmission Path Stability Index
TSO	Transmission System Operator

1

Introduction

The continuous demand of electric power entails a growing number of challenges in the development of modern power systems. The production of electric power is seldom located close to where the consumption of electricity is located. This increases the complexity of a reliable power transfer and is the result of both economical and environmental pressure, which is compensated for by operating the power system close to the limits of stability [1, 2]. A large and highly interconnected power system connected to loads that varies throughout the day and which operates close to its limits during certain periods of time will be defined as a stressed network [2]. When contingencies occur at this stage, voltage instability and in worst case voltage collapse is likely to occur [2]. Protecting the power system from voltage collapse is essential for providing a reliable power transfer and to be able to ensure that precautions are taken when a contingency occur. A voltage collapse can result in the entire systems shutting down, which leads to extensive economical consequences and unsatisfied customers [3]. The vitality in detecting an imminent voltage collapse and take fast corrective actions to prevent it is of great importance in order to maintain stability [1, 2]. One way to obtain this is to implement a system protection model based on system stability indicators [4]. These types of models are still in a stage where not as much research is done for an operational implementation in the power system and the efficiency is still being evaluated by means of simulations. In such simulations the model utilizes system protection schemes (SPS) which are initialized to protect the system if there are tendencies to voltage instability [1, 2, 4].

1.1 Problem

This thesis is supposed to result in an investigation of how to detect a voltage collapse by means of system stability indicators such as different voltage stability indicators together with signals from over-excitation limiters (OELs). The information necessary for calculating these indicators is measured locally at each bus and/or are extracted from a supervisory control and data acquisition system (SCADA) supported with phasor measurement units (PMUs). These signals can be processed and used to monitor the trends which may point towards a voltage instability. The indicators give an overview of weak load buses in the system and can be used as a basis for initializing SPSs to prevent a voltage collapse. Such methods could for example be increasing AVR set-points to prevent OELs to be activated, shunt compensation such as Static Var Compensators (SVC) or shedding of load. Based on the signals obtained from indicators and OELs, a method to process these are proposed. The signals are to be processed in a system protection model which takes the corrective actions automatically in terms of where, when and how much preventive actions are to be taken.

1.2 Purpose of the thesis

The purpose of the thesis is to develop and implement a system protection model for the Nordic 32-bus test system [5] in PSS/E [6] in order to foresee and prevent voltage collapse. The system protection model will be based upon voltage stability indicators and signals from OELs which are used to predict and prevent possible voltage collapse scenarios in an interconnected power system.

1.3 Delimitations

This thesis will investigate the usage of voltage stability indicators when designing system protection models. The voltage stability indicators will be investigated in PSS/E and the most suitable indicator for the purpose of the protection model will be implemented. The design of the model algorithms in PSS/E will be based on these indicators and information from OELs signals from the synchronous generators. The following limitations are set:

- The system protection model will be implemented and tested for the Nordic32 test system, a generic model for any power system network will not be developed.

- The model for system protection will not include all possible mitigating actions.
- The impact of transients occurring in measured quantities used for the calculations of the indicators will not be investigated.

1.4 Method

The problem is broken down into a number of specified tasks which are necessary in order to design the system protection model. The work mainly involves simulations in PSS/E. The simulations were run and automated by the use of Python scripts [6, 7] to increase speed and keep the simulations consistent. Furthermore, the system protection model which will be incorporated in PSS/E will be developed in the imperative programming language Fortran [8]. The specified tasks are listed below in chronological order:

- Literature studies on voltage instability, collapse and system stability indicators as well as methods to prevent a voltage collapse.
- Simulations in PSS/E of a two and a three-bus system to get an understanding of different voltage stability indicators as well as learning how to control PSS/E with Python scripts in order to do simulations faster and to keep the simulations consistent.
- Perform simulations on the Nordic32 test system and extract measurement data to base the calculations of the voltage stability indicators on using Matlab.
- Analysis of the result in Step 2 and 3 above in order to be able to develop a method of how to prevent voltage collapse by using the information from indicators.
- Develop a system protection model based on the method developed in step 4 using Fortran and implement the model in PSS/E.
- Perform simulations in the Nordic32 test system with the system protection model implemented to evaluate indicator characteristics compared to the result obtained from Matlab [9] (Step 3) and automatic mitigating actions.
- Perform case studies designed to cause a voltage collapse in the Nordic32 test system and evaluate how the models can prevent the collapse.

1.5 Thesis outline

This thesis is divided into four chapters beyond the present one. The content of these four chapters are summarized in the bullet list below:

- Chapter 2 contains the theoretical background on which this thesis is based on.
- Chapter 3 contains three case studies designed to evaluate the performance of the voltage stability indicators and how these react to different dynamic scenarios. The three case studies consists of a two-bus system, a three-bus system and on the Nordic32 test system.
- Chapter 4 contains the functionality, implementation and evaluation of the system protection model of how well it can prevent a voltage collapse in the Nordic32 test system.
- Chapter 5 contains the conclusions which can be drawn from the result presented in this thesis as well as suggestions for future work that can be done to improve the result.

2

Technical Background

Modern power systems are getting more and more automated, both for the purpose of monitoring and for taking mitigating actions. These mitigating actions should leave as much as possible of the network still operational when a contingency occur [10]. Power system protection comprises different components protecting specified parts in the network. However, this report will focus on and investigate system protection models and schemes monitoring voltage stability in the network and the way it processes local bus data measured by current transducers and voltage transducers (VT) [11]. The data provided by the transducers are processed to calculate voltage stability indicators and based on these indicators, algorithms will automatically determine when, where and how mitigation actions are taken. Theory that addresses the advantage of using a system protection model and its implementation as a model in PSS/E will be discussed in this section.

2.1 Voltage stability

Voltage stability is not something new for the transmission system operators (TSOs). As a consequence of the major grid blackouts caused by voltage instability in North America and Europe during the year of 2003 the topic has been given more attention [12]. Together with an increasing demand of electricity, increasing load rates and a more complex level of power system control, monitoring voltage stability constitutes a more important role for the PSOs [2]. The higher level of complexity is a result of that more compensating equipment, such as SVCs, are installed and used in order to handle longer transmission paths since most power is produced far from where it is consumed [13].

2.1.1 PV and VQ curves and system stability

The characteristics of power transfer and voltage stability in a power systems can be described by P-V and V-Q curves, where P is active power, Q reactive power and V the voltage. The characteristics depend on multiple factors, such as transmission line impedance, power factor, injected reactive power and the power consumed by loads. These factors can dynamically be altered, meaning that the curves will change, for example if there is a loss of transmission lines due to faults or change in power factor of the load [14]. The PV-curve equation can be expressed by combining the following two power transfer equations for a two bus system and solving it for the receiving end voltage, V . Here, E is the sending end voltage, X the line impedance and δ the voltage angle.

$$P_r = -\frac{EV}{X}\sin(\delta) \quad (2.1)$$

$$Q_r = \frac{VE\cos(\delta) - V^2}{X} \quad (2.2)$$

This gives the following equations which can be used to describe both the PV-curve and the VQ characteristics for reactive compensation.

$$V = \sqrt{\frac{E^2}{2} - QX} \pm \sqrt{\frac{E^4}{4} - X^2P^2 - XE^2Q} \quad (2.3)$$

The maximum active power transfer with the corresponding voltage can be found through the fact that the equation only has one solution at this point, whereas it for $P < P_{max}$ has two. This yields the following two equations which corresponds to the PV-curves "tip of the knee" as seen in Fig. 2.1a [14].

$$P_{max} = \frac{1}{X} \sqrt{\frac{E^4}{4} - XE^2Q} = \frac{E^2}{2X} \frac{\cos(\phi)}{1 + \sin(\phi)} \quad (2.4)$$

$$V_{P,max} = \sqrt{\frac{E^2}{2} - XQ} = \frac{E}{\sqrt{2}} \frac{1}{\sqrt{1 + \sin(\phi)}} \quad (2.5)$$

The equations can also be expressed as a function of the power angle ϕ (2.4) and (2.5) also characterize the boundary for voltage stability and instability operation. By replacing the Q with $(Q_L - Q_C)$ where Q_L is load reactive power and Q_C is the

compensated reactive power in (2.3), the VQ-characteristics can be explained by the following equations [14].

$$Q_{C,min} = Q_L - \frac{E^2}{4X} + \frac{XP^2}{E^2} \quad (2.6)$$

$$V_{Qc,min} = \sqrt{\frac{E^2}{4} + \frac{X^2P^2}{E^2}} \quad (2.7)$$

These indicate the minimum point of the VQ-curve seen in Fig. 2.1b which is defined for a constant $P+jQ$ load. A PV-curve for a constant power factor with no injected reactive power and a VQ-curve with a constant load can be seen in Fig. 2.1. The curves is for an ideal case with no line charging or resistance and with a constant power factor[14].

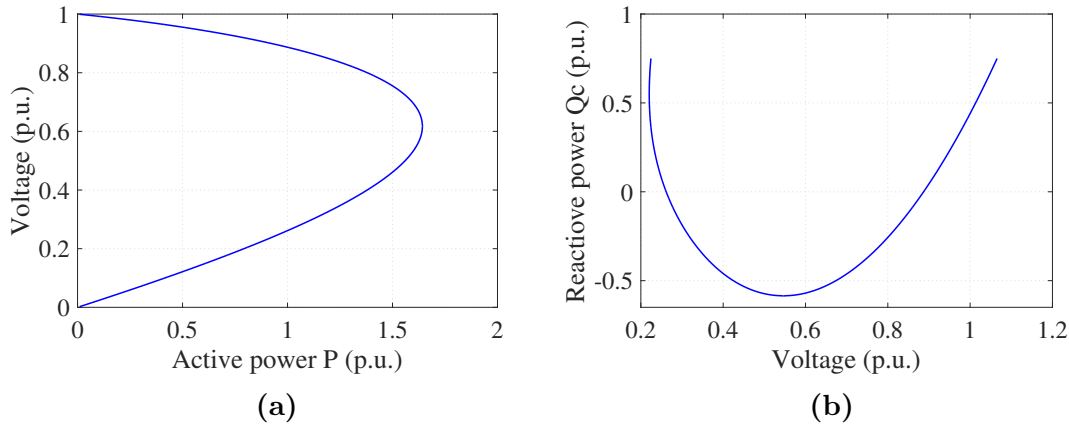


Fig. 2.1: PV and VQ curves illustrating a system with a constant power factor, with no injected reactive power and with a constant load. **(a)** Voltage as a function of transferred active power with a constant power factor and with no injected reactive power. **(b)** Voltage as a function of transferred reactive power with a constant load.

2.1.2 The effects of contingencies on voltage stability

If a fault or a scenario that can cause a transmission line to be tripped take place, voltage stability can heavily be affected due to the loss of power transfer capability because of an increasing transmission line impedance. A basic ideal case can be seen in Fig. 2.2 where three lines are connected in parallel between two buses, as well as two lines and one single line [14][15].

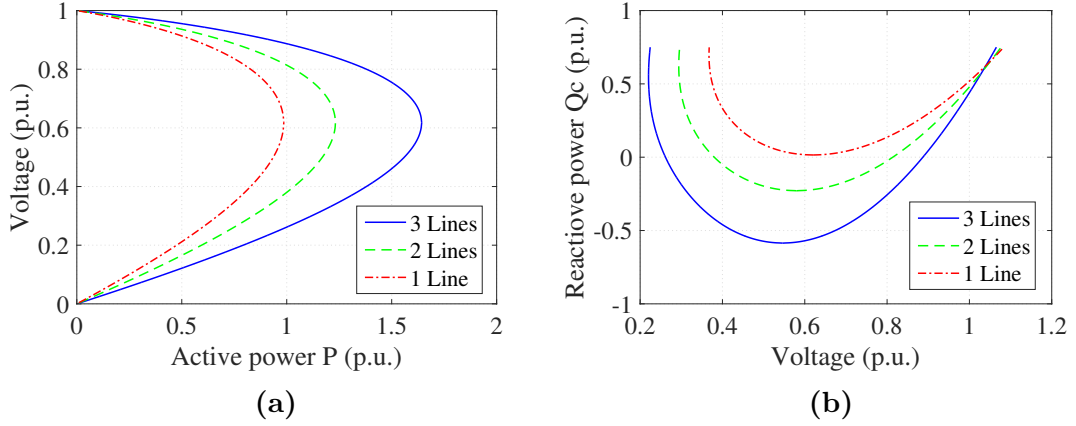


Fig. 2.2: The characteristics of PV and QV curves when one, two or three lines carries the power transfer between two buses. **(a)** Voltage as a function of transferred active power as the operating point for the voltage decreases with less lines in parallel. **(b)** Voltage as a function of transferred reactive power as reactive power losses is affected with less lines in parallel.

The increase of transmission line impedance changes the PV-characteristics which is seen in Fig. 2.2a. For a given load, the voltage will find a new operating point with less active power transfer. This, will result in higher requirement of reactive power at the generator and a higher reactive compensation to increase the operating point for the voltage and this is illustrated in Fig. 2.2b. If the system is operating close to the limit it is also possible that the bus can become unstable.

2.1.3 Reactive power compensation

Capacitive shunt compensation in form of fixed shunts can increase the maximum power transfer by increasing the bus voltage by means of injecting reactive power. Therefore the margin to voltage instability is also increased. The amount of injected reactive power is square-proportional to bus voltage, thus is the available shunt compensation less when the voltage is lower and vice versa. The injected power Q_C is determined by the following equation, where V is bus voltage and X_{Sh} is the shunt reactance [15][14].

$$Q_C = \frac{V^2}{X_{Sh}} \quad (2.8)$$

The Nordic32 test system, which is used for the purpose of the subject of this thesis only includes fixed shunts which is why only this method is covered in this section. With this said, the above equation concludes that a fixed shunt cannot be used for voltage control but only for voltage support. The steady state operating voltage can be found where the VQ-curve intersects the shunts characteristic curve as seen in Fig. 2.3. A disturbance leading to a change in the balance of active and reactive power as well as impedance will result in a change of the VQ-characteristics, thus moving the operating point [15].

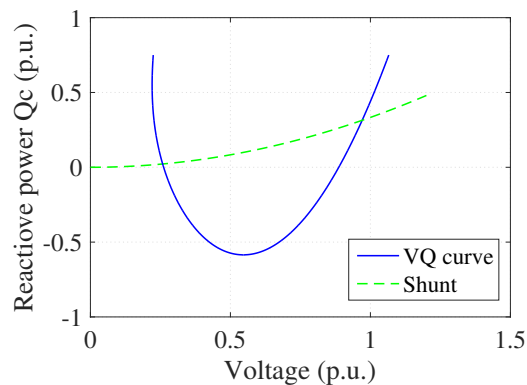


Fig. 2.3: Reactive power as a function of voltage and the associated shunt compensation as a function of voltage.

2.1.4 Online load tap changers (OLTC)

OLTCs are used for frequent regulation of reactive power, and thus load voltage. They can be used for regulating the voltage level in, for example a low voltage distribution area to keep constant voltage in the load area. OLTCs can therefore have a significant effect on voltage stability, due to the change in admittance and reactive power flow during tap changing operation [16]. A π -model for an OLTC can be seen in Fig. 2.4, which consist of a series admittance y_t that is dependent on the tap-ratio a . Tap changing operation change the value of the tap-ratio and thus the voltage difference between the main and secondary sides of the transformer. The voltage difference can typically be adjusted to $\pm 10\%$ of the nominal value [15, 16].

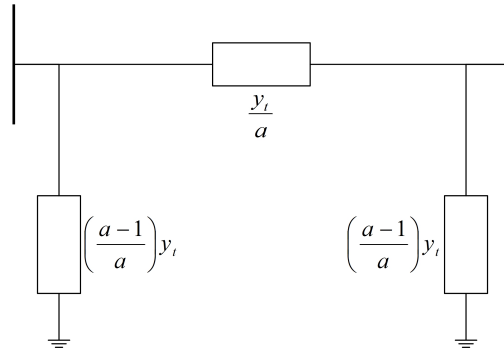


Fig. 2.4: π -model of a OLTC with series admittance y_t and tap-ratio a .

2.1.5 Over excitation limiters (OEL)

In case of a decrease in voltage, generators can be used as AVR's to increase the production of reactive power and thus increase voltage. An increase in reactive power output is achieved by an increase in field winding current. However, higher reactive power production than what the machine is designed for can be harmful for the field windings and can possibly overheat the machine. If this happens the OEL of the generator is activated and thus preventing change in the field current (and reactive power generation). This will result in losing control of the voltage regulation at the generator terminal E_t and a constant voltage is instead found at E as seen in Fig. 2.5 [14, 15].

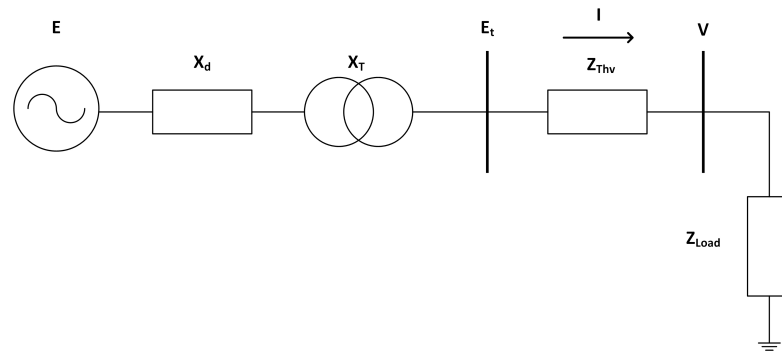


Fig. 2.5: Equivalent circuit of a two bus network showing the generator reactance X_d which is added in series with X_T and Z_{Thv} when the OEL is active, thus increasing the impedance.

When this happens the total impedance of the generator seen from the receiving end bus will change. The generator direct axis reactance X_d will thus be added in series with the generator transformer reactance, instead of only consist of the transformer reactance as when the OEL is inactive. The result is a higher impedance seen from the bus and when this happens the network is weakened. Furthermore a reduction in maximum power transfer is enforced and the bus voltage tend to decrease [15]. The signal from OEL activation at generator buses is therefore critical for determining the systems stability margin to unstable operation.

2.1.6 Voltage instability and voltage collapse

Voltage instability and voltage collapse may be defined in several ways depending on organization. Conseil International des Grands Réseaux Électriques (CIGRÉ, International Council on Large Electric Systems) and IEEE use their own formal definitions, but with a common characterization that can be compiled with the explanation given by P. Kundur: *"Voltage collapse is the process by which the sequence of events accompanying voltage instability leads to a low unacceptable voltage profile in a significant part of the power system."* [15].

Voltage instability on the other hand can be defined as: *"voltage instability stems from the attempt of load dynamics to restore power consumption beyond the capability of the combined transmission and generation system."* [13].

Propagation time for this type of instability problems can both be short-term and long-term. Short-term voltage instability is the cause of fast dynamic behavior from electronically controlled loads while long-term voltage instability is a result of slow acting regulating equipment such as tap-changers etc. [17].

2.1.7 Causes of voltage instability

A power system is subject to different types of voltage instability during regular operation and there are many possible causes of voltage instability that can lead to a voltage collapse [17]. Both voltage and voltage angle have an impact on the stability of a network and instability in one of them can lead to instability in the other. At the same time, a solution for one of them may not be the solution for the other [18].

Areas in the power system with a high density of loads are often a victim of voltage instability. While areas remote from the load, that are exposed to voltage instability has an angle instability problem [13]. With this said, voltage instability

is mainly caused by loads, since the power consumed by them are often restored by regulating measures. Such measures are for example tap-changing transformers whose operation often increases the reactive power above the capability point of the system which tend to stress the system [17]. Meshed network tend to be extra vulnerable when lines or generators are down for service. Maintenance work at critical areas of the network cause stress in the system and make it much weaker than during normal operation [17]. Contingencies at this stage often lead to voltage instability which is difficult to compensate for without quick protection schemes that are able to prevent instability escalation [17].

2.2 Previous work on voltage stability indicators

Voltage stability analysis is getting more and more attention in literature due to the growing demand of the PSOs to foresee voltage instability in order to ensure reliable electricity distribution. The use of voltage stability indicators have the advantage of easily monitoring how close the system is to a voltage collapse which in other words can be seen as a way to estimate how much power the system are able to supply the loads without endangering the stability of the system. Monitoring voltage stability margins can be done by many methods [19]. There are a lot of research carried out on the topic of voltage stability indicators. A good guide to the topic is the work done by the IEEE Power and Energy Society in the report *Voltage stability and assessment: concepts, practices and tools* [19]. Here, the basic concepts are explained and the advantages and disadvantages with different indices compared to conventional methods for monitoring voltage stability are listed. Further, a more overall comparison of different voltage stability indicators was conducted by the master's thesis student Vegar Storvann at Norwegian university of science and technology-Trondheim (NTNU) [4]. In the Norwegian report a thorough investigation is done for six voltage stability indicators. The performance of the indicators are investigated in different network setups and the result of this investigation is the underlying reason for the choice of indicators used in this report.

2.3 Voltage stability indicators

Four of the voltage stability indicators investigated in [4] mentioned in Section 2.2 are further examined in this report. These indicators are impedance stability

index (ISI), transmission path stability index (TPSI), s-difference indicator (SDI) and fast voltage stability index (FVSI). These four indicators are explained below, followed by an comparison of advantages and disadvantages when choosing the most suitable indicators for the purpose of this thesis. The indicators are used as pointers to find the weakest bus in the network and these buses have often loads connected to them.

2.3.1 Impedance stability index (ISI)

ISI is based on the maximum power transfer of a circuit. The maximum power transfer of the simple circuit in Fig. 2.6 occurs when the thévenin impedance Z_{Thv} equals the load impedance Z_{Load} and can easily be derived by taking ohm's law of the circuit [20]

$$I = \frac{E_t}{Z_{Load} + Z_{Thv}} \quad (2.9)$$

and finding the voltage across Z_{Load} .

$$V_j = E_t \frac{Z_{Load}}{Z_{Load} + Z_{Thv}} \quad (2.10)$$

The power dissipated by the load is then described by

$$P_{Load} = V_j I \cos(\delta) = E_t^2 \frac{Z_{Load}}{(Z_{Load} + Z_{Thv})^2} \cos(\delta) \quad (2.11)$$

which can be rewritten as

$$P_{Load} = \frac{E_t^2}{Z_{Load} \left(\frac{\sqrt{Z_{Load}}}{\sqrt{Z_{Thv}}} + \frac{\sqrt{Z_{Thv}}}{\sqrt{Z_{Load}}} \right)^2} \cos(\delta) \quad (2.12)$$

which has its maximum value when $Z_{Thv} = Z_{Load}$ or in other words, when the voltage drop over Z_{Thv} is equal to the voltage drop over the Z_{Load} . This also implies that the maximum power transfer and therefore the voltage instability critical point is reached when

$$ISI = \frac{|Z_{Thv}|}{|Z_{Load}|} = 1 \quad (2.13)$$

If the ISI is less than one, the voltage at the bus is stable. If instead greater or equal to one, the voltage profile is unstable. A value of 0.8 is discussed to be a good indicator value for alarm [4, 21].

Thévenin equivalent estimation methods

In this report two methods of estimating the thévenin impedance of a meshed network are used, these are described below.

Method 1: Estimation by local bus measurements

The use of thévenin's theorem enables any one-port circuits to be modeled as a single voltage source with a equivalent impedance. One way to implement this approach and to estimate the parameters of the simple power system network seen in Fig. 2.6 is presented below [20, 22].

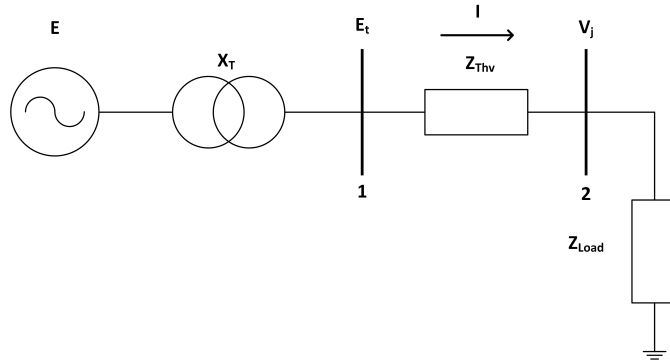


Fig. 2.6: Thévenin equivalent of a simple power system network.

This method is based on consecutive measurements of the complex quantities voltage V_j and current I at the load bus. The measurements are used to find the unknown thévenin voltage E_t and the thévenin impedance Z_{Thv} in

$$E_t^{(t)} = V_j^{(t)} + I^{(t)} Z_{Thv}^{(t)} \quad (2.14)$$

This equation has an infinite number of solutions but one way to get around this problem is to perform consecutive measurements of V_j and I and assuming that E_t and Z_{Thv} are constant. If these assumptions are made it is possible to say that

$$\begin{aligned} E_t^{(t)} &= E_t^{(t+1)} \\ Z_{Thv}^{(t)} &= Z_{Thv}^{(t+1)} \end{aligned}$$

which result in that the following connection are valid:

$$V_j^{(t)} + I^{(t)} Z_{Thv}^{(t)} = V_j^{(t+1)} + I^{(t+1)} Z_{Thv}^{(t+1)} \quad (2.15)$$

and solving for $Z_{Thv}^{(t+1)}$ gives

$$Z_{Thv}^{(t+1)} = \frac{V_j^{(t)} - V_j^{(t+1)}}{I^{(t+1)} - I^{(t)}} \quad (2.16)$$

which will be an estimation of the thévenin impedance of the network seen by the bus [20].

Method 2: Estimation by admittance matrix

Another way to estimate the thévenin impedance of a interconnected power system is to use the admittance matrix of the network which can be obtained from SCADA. To illustrate this method the simple two bus system in Fig. 2.6 is used as an example. The associated admittance matrix for this system becomes

$$Y = \begin{bmatrix} Y_{11} & Y_{12} \\ Y_{21} & Y_{22} \end{bmatrix} = \begin{bmatrix} \frac{1}{Z_{Thv}} & -\frac{1}{Z_{Thv}} \\ -\frac{1}{Z_{Thv}} & \frac{1}{Z_{Thv}} \end{bmatrix}$$

which can be inverted to its impedance matrix $Z = Y^{-1}$ where the diagonal elements will form the thévenin impedance seen by the bus [23]. However, matrix inversion procedure for larger power system networks may need a large amount of computational power. By modifying the admittance matrix by adding the load impedance Z_{Load} and generator impedance X_d (Fig. 2.5) to the self admittance of each bus it is possible to make an estimation of all the thévenin impedance in the system with only one inversion of the admittance matrix instead of doing it for each bus [23].

$$Y = \begin{bmatrix} \frac{1}{Z_{Thv}} + \frac{1}{X_T} & -\frac{1}{Z_{Thv}} \\ -\frac{1}{Z_{Thv}} & \frac{1}{Z_{Thv}} + \frac{1}{Z_{Load}} \end{bmatrix}$$

The self impedance obtained from this admittance matrix however, will include the load impedance which is not the quantity used for the ISI calculation. What is obtained from the diagonal elements in this matrix is illustrated in Fig. 2.7 [23].

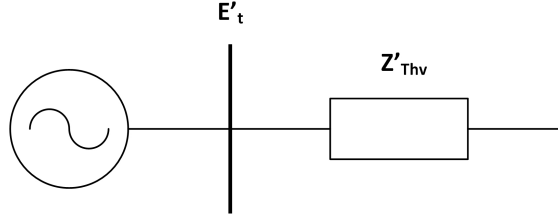


Fig. 2.7: Thévenin equivalent illustrating the thévenin impedance Z'_{Thv} which includes the load impedance.

By comparing Fig. 2.6 and Fig. 2.7 one can conclude that Z'_{Thv} is the result of paralleling Z_{Thv} and Z'_{Load} which implies that

$$Z_{Thv} = \frac{Z_{Load}Z'_{Thv}}{Z_{Load} + Z'_{Thv}} \quad (2.17)$$

which makes it possible to extract the Z_{Thv} used in the calculation for ISI [23].

2.3.2 Transmission path stability index (TPSI)

TPSI is based on (2.5) which describes the voltage magnitude of which maximum power transfer occur. Inserting the receiving-end reactive power equation (2.2), gives the following equation,

$$TPSI = \frac{V_s}{2} - (V_s - V_r \cos(\delta)) \quad (2.18)$$

which when equals zero, indicates the maximum power transfer operation point or the stability/instability boundary at the knee of the PV-curve [4, 24].

This indicator is like the ISI based upon that the maximum power transfer occurs when the voltage drop over the line equals the drop over the load. The voltage drop over the line $V_s - V_r \cos(\delta)$ can be illustrated with phasors as in Fig. 2.8. Where V_s and V_r is the sending and receiving end voltage with the angle difference δ for a two bus system. The TPSI does not however, use the thévenin equivalent

compared to the ISI but only the voltage at the sending end, receiving end and the voltage angle difference for a two bus system [24]. The voltage and angle measurement needs to be synchronized.

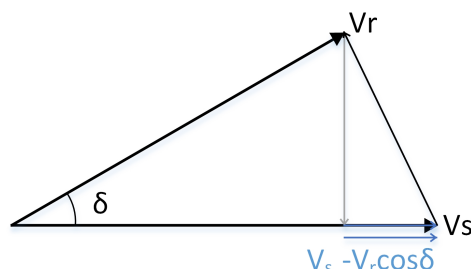


Fig. 2.8: Voltage drop $V_s - V_r \cos \delta$ between sending end and receiving end projected on the sending end bus voltage phasor V_s .

For the two bus system the indicator can easily be calculated with (2.18), for larger system however, all paths need to be taken into account. The weakest path will then determine the margin to a voltage collapse. This is due to that if one transmission path moves past the maximum transmission point, it will put higher stress on the other transmission paths. Each transmission path can be seen as a radial network with the bus furthest away from the generating bus being the bus which is most exposed to voltage instability. In addition, the effect of each bus along the path needs to be taken into account as they can contribute to keeping the path stable. An active power transmission path is defined as a sequence of buses with decreasing voltage angle between each bus, in essence the direction of active power flow [4, 24]. The voltage drop along a path can be explained by the phasor-diagram seen in Fig. 2.9. Where $\Delta V'_d$ is the sum of the sequence of voltage drops along the transmission line, where each voltage drop for each voltage vector is projected on the previous voltage vector [24]. Each voltage drop is then projected on the starting bus, which results in the voltage drops ΔV_{d12} , ΔV_{d23} and ΔV_{d34} seen from the sending end bus with the voltage phasor V_1 . The sum of these voltage drops results in $\Delta V'_d$ which is the voltage drop over the transmission path. The condition for maximum power transfer and voltage instability for a radial or meshed network is therefore when

$$\Delta V'_d = \frac{V_1}{2} \quad (2.19)$$

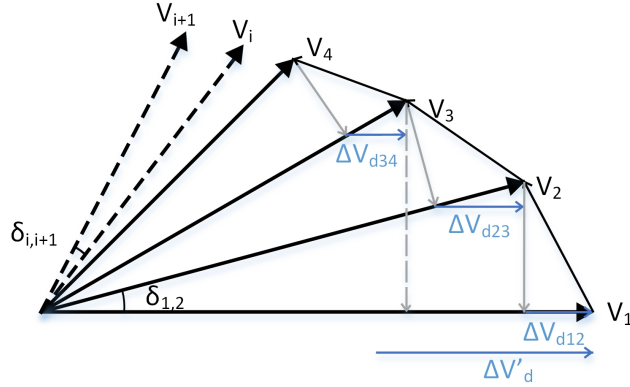


Fig. 2.9: Voltage drops of a transmission path projected on the sending end bus voltage phasor V_1 . Resulting in a sum of voltage drops $\Delta V'_d$

The Transmission path stability index for a n -bus transmission path can be calculated as the receiving end voltage subtracted by the sum of all voltage drops between each bus according to the following equations.

$$\Delta V'_d = \sum_{i=1}^{n-1} (V_i - V_{i+1} \cos(\delta_{i,i+1})) \cos(\delta_{1,i}) \quad (2.20)$$

$$TPSI = \frac{V_1}{2} - \Delta V'_d \quad (2.21)$$

Where V_1 is the first bus in a transmission path, $\delta_{i,i+1}$ is the voltage angle between two given buses in the transmission path, and $\delta_{1,i}$ is the voltage angle between the first bus and a given bus of a transmission path [24].

This calculation needs to be preformed for each path in the system to be able to find the weakest path and thus be able to determine the system voltage stability margin [24]. Previous work states that for meshed networks, there is not enough evidence that proves that a TPSI value of zero corresponds to voltage instability/collapse due to that a bus is stable as long as there is one stable path. This implies that for a meshed network, the TPSI can reach below zero while maintaining voltage stability. However, due to the increased stress on other paths when the weakest path becomes unstable, simulations have proven that it serves well as an estimation method for voltage stability [4]. Previous work states that reactive power flow paths also needs to be considered when finding the lowest TPSI. This is achieved by using the same method and equations but with the exception of instead

choosing paths with decreasing bus voltage magnitude instead of bus voltage angle [4, 24].

To find the weakest transmission path, Dijkstra's algorithm of finding the least weighted path in a directional graph can be used. This as the active power flow is directional and each branch will have a certain "weight" (increase in voltage angle and change in voltage magnitude). Dijkstra's algorithm assumes that both the starting and ending bus is known, however in this case, the bus with the lowest TPSI value is unknown (ending bus) and only the starting bus is known [25]. Therefore the algorithm is modified to find all paths to buses which have lower voltage angle than all connected buses. Through this the lowest TPSI value for the weakest bus can be found, and also enables the possibility to find other buses with low TPSI values.

The algorithm is based on the use of two arrays called *stack* and *visited* to find paths. The visited-array is used for making sure that each path is only considered and calculated once. The stack-array is used for storing a path as a sequence of nodes and in the end calculating the TPSI. Considering the directed graph in Fig. 2.10, there are four different paths from node one to seven which all need to be found if they are to be compared. The algorithm both have to find the green and red path which share paths from node one to two, as well as it has to take into account that the green and yellow paths share the last part between node six and seven.

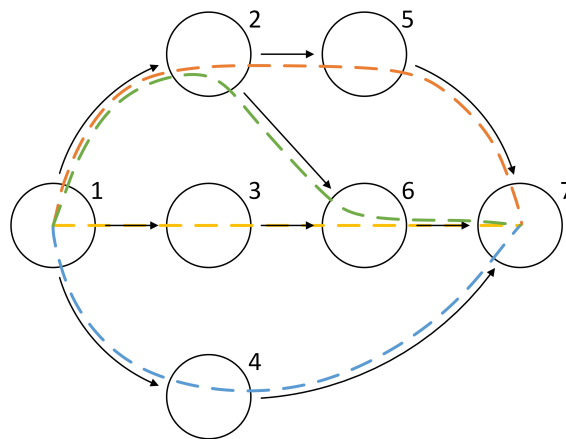


Fig. 2.10: Directed graph with four different possible paths from node one to seven.

A solution of how the problem can be solved is stated in the following list, starting at node 1:

1. Node 1 is put in the Visited-array as well as in the Stack-array. Since either one of node 2, 3, 4 are in the Visited-array, the path can therefore continue with node 2.
2. When the algorithm has reached node 2 the two arrays (Stack and Visited) will both contain node 1 and 2, continue with node 5.
3. At node 5 the two arrays Visited and Stack will contain 1, 2, 5 and 1, 2, 5 respectively. Continue with 7 where the red path is found and TPSI can be calculated. When reversing to node 2, node 5 and 7 are removed from Stack but only node 7 from Visited is removed so that the algorithm does not continue with node 5 again.
4. Next step is to continue from node 2 to 6, the arrays will contain nodes 1, 2, 5, 6 and nodes 1, 2, 6 for Visited and Stack respectively.
5. Continuing with node 7, comprising the green path. When the algorithm revert back to node 2, it will find that both node 5 and 6 are in the Visited array. At this point the algorithm have to revert back to node 1, removing node 2, 6, and 7 from the Stack but only nodes 5, 6 and 7 from Visited.
6. Since either one of node 3, 6 and 7 are now found in visited, this also forms the yellow path in similar way. When reverting back to node 1, the Visited array will contain node 1, 2 and 3 and the Stack will contain node 1 again.
7. In the end, when the blue path is found, the Visited array will contain 1, 2, 3 and 4 thus leaving no more options. At this point all paths are found.

The TPSI can be calculated at each time a new path is found and compared to the previous calculated TPSI value in order to find the path with the lowest TPSI. Several ending nodes can be found using this method, as the graph is directed. An ending node is seen as a graph with no direction leading from it. This can be applied to power systems as the power flow is directional.

2.3.3 S-difference indicator (SDI)

The SDI is just as the ISI based on local bus measurements. Two consecutive measurements of the apparent power at the receiving end on a line is done. Voltage instability for this indicator occur when the change in apparent power at the sending and receiving end is zero, $\Delta S=0$. In other words, when an increase in apparent power at the sending end no longer yields an increase in receiving end apparent power due to an increase in losses along the line. Increasing losses along

the line occur when the line is heavily loaded and starts to consume more and more reactive power [26].

If the apparent power at the receiving end is given by

$$S_j^{(t)} = V_j^{(t)} I_{ij}^{(t)*} \quad (2.22)$$

Where the subscripts i and j constitutes different buses. The difference between the two consecutive measurements is written as

$$\Delta V_j^{(t+1)} = V_j^{(t+1)} - V_j^{(t)} \quad (2.23)$$

$$\Delta I_{ij}^{(t+1)} = I_{ij}^{(t+1)} - I_{ij}^{(t)} \quad (2.24)$$

This yields an apparent power at the following time steps as

$$S_j^{(t+1)} = S_j^{(t)} + \Delta S_j^{(t+1)} = (V_j^{(t)} + \Delta V_j^{(t+1)})(I_{ij}^{(t)} + \Delta I_{ij}^{(t+1)})^* \quad (2.25)$$

which can be simplified to and rewritten as the critical condition below.

$$\Delta S_j^{(t+1)} = \Delta V_j^{(t+1)} I_{ij}^{(t)*} + V_j^{(t)} \Delta I_{ij}^{(t+1)*} = 0 \quad (2.26)$$

If this criterion is met it means that the receiving end apparent power flow no longer increases even though more power is transmitted from the sending end. Separating the angle between the two terms the SDI indicator can be defined as:

$$SDI = 1 + \left| \frac{I_{ij}^{(t)*} \Delta V_j^{(t+1)}}{V_j^{(t)} \Delta I_{ij}^{(t+1)*}} \right| \cos(\delta) \geq 0 \quad (2.27)$$

A stable voltage profile occurs when $SDI \geq 0$ and can only be trusted when the line actually consumes reactive power [4].

2.3.4 Fast Voltage Stability Index (FVSI)

The FVSI is in its simplest form based on measurements of sending end voltage and reactive power at the receiving end, as well as known characteristics of the

line. The two bus system in Fig. 2.11 can be used to explain the principle. The current equation between two buses is used as starting point [27].

$$I = \frac{V_i - V_j}{R + jX} \quad (2.28)$$

The apparent power at the receiving end j can be found by multiplying the the current I with the receiving end voltage V_j [4].

$$S_j = V_j I = P_j + Q_j \quad (2.29)$$

If the reactive power Q_j is extracted from the apparent power and rewritten as a second-order equation for U_j the following is obtained

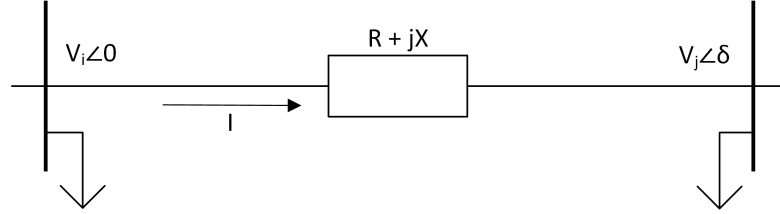


Fig. 2.11: Two bus system used to explain FVSI, V_i and V_j are sending and receiving end voltage and I the current flowing in the line with characteristics $R + jX$ between the two load buses.

$$V_j^2 - V_i V_j \left(\frac{R}{X} \sin(\delta) + \cos(\delta) \right) + \left(X_{ij} + \frac{R^2}{X} \right) = 0 \quad (2.30)$$

As long as there is only real solutions for the second-order equation the system is stable, which is how the FVSI is defined [27].

$$V_j = \frac{\left(\frac{R}{X} \sin(\delta) + \cos(\delta) \right) V_j \pm \sqrt{\left[\left(\frac{R}{X} \sin(\delta) + \cos(\delta) \right) V_i \right]^2 - 4 \left(X + \frac{R^2}{X} \right) Q_j}}{2} \quad (2.31)$$

Solutions of the above equation that corresponds to only real solutions are described by

$$\frac{4Z^2Q_jX}{(V_i)^2(R\sin(\delta) + X\cos(\delta))^2} \leq 1 \quad (2.32)$$

For these roots, the angle difference δ is very small, which results in the following expression

$$FVSI_{ij} = \frac{4Z^2Q_j}{V_i^2X} \quad (2.33)$$

Which will indicate a stable voltage profile as long as $FVSI_{ij} \leq 1$

2.3.5 Indicator comparison

The four indicators explained under Section 2.3 have different characteristics and are suitable for different types of applications. These indicators are based on local and wide area measurements by PMUs [28]. The comparison below is mainly based on the work done by Vegar Storvann mentioned in Section 2.2. The focus of this comparison is oriented towards the discussion on advantages and disadvantages by V. Storvann and not necessarily on the results presented in the report.

The ISI which is defined by the ratio between the load impedance Z_{Load} and the thévenin impedance Z_{Thv} involves two common methods to calculate the thévenin impedance, both explained in Section 2.3.1. Using consecutive measurements (method 1) as is done in (2.16) has the drawback of creating a noisy signal, due to small variations during steady state operation [4]. Using the admittance matrix of the system (method 2) on the other hand has the advantage of a more stable calculation of the thévenin impedance even though the computational calculation are more demanding [23]. The TPSI is based on wide area monitoring where the weakest path from the strongest bus in the system to the weakest bus, is found and evaluated. V. Storvann proposes that a path finding algorithm needs to be implemented in meshed network to find all possible paths in order to ensure that all combinations are analyzed [4]. SDI is like the ISI based on consecutive measurements and is subject to the same noisy signal at steady state operation. FVSI which depend on both PMU measurements and branch characteristics show the worst result during stable conditions as well as during contingencies and which performance was categorized as *"does not provide any useful information"* [4].

2.3.6 Choice of voltage stability indicators

Two of the indicators compared in Section 2.3.5 were decided to be further investigated and evaluated for the purpose of the protection model designed in this thesis. These indicators are the ISI and the TPSI. This choice was based on the opportunities to further develop the performance of the indicators and their reliability. The ISI had the advantages of calculating the thévenin impedance by using the system admittance matrix which makes it more stable at the same time as it was performing well during both steady state operations and contingencies. The TPSI had a lot of development potential when it comes to the path finding algorithm. Extending the indicator with implementing the algorithm would make it a more reliable and make a good candidate for a wide area indicator.

2.4 Preventing voltage collapse

If a power system is operating close to its limits and voltage instability is likely to occur, preventive measures must be taken. This can be done in several ways depending on situation and available compensation devices.

The main idea of voltage control is to control the production and absorption of reactive power in the network [17]. Three mitigating methods are further discussed in this report, these are load shedding, exciter control by increasing the AVR set-point and FACTS devices.

2.4.1 Load Shedding

Shedding of load is an efficient method to prevent voltage instability and collapse due to that it imitatively decreases the stress on the system. In a system protection scheme, load shedding is seen as the last measure to prevent a power system collapse but is a daily procedure in many developing countries [29].

There are different approaches to when, where and how much to shed loads in a power system. On method to shed load automatically is described in [30]. This paper proposes a method to find the minimal shedding that have the least impact on the system but still is enough to save it from further instability. Further are this method optimized based on shedding delays and location of shedding and in the end are a method to find and optimize controller parameters for achieving an automatic load shed [30]. Another method described in [31] covers the use of

Generation Shift Factors (GSF) for which the sensitivity is calculated to find the most optimal loads to shed in terms of location and amount [31].

2.4.2 Exciter control and increasing AVR set-point

Synchronous machines with AVRs is one of the key stones of an active voltage control. Clever use of AVRs can help to prevent the activation of OELs in order to prevent these from activating or to "buy time" until this happens by increasing reactive power production from other generators. Delaying the activation of the OEL has the advantage of buying more time that can be used to take further preventive measures. Such measures could be to activate compensating devices and by this measure prevent a voltage collapse [14, 17].

The idea behind using the AVR to regulate the voltage set-point in a power system, where most machines have the feature installed, is to increase the set-point at nearby buses whenever a triggering event at one or many machines occur. Such triggering events can be that the OEL is close to activation or has already been activated. If the voltage set-point is increased within a safe level at all nearby buses, these machines will start to increase their reactive power production resulting in an decrease of reactive power production at nearby voltage controlling equipment. The reactive power production is therefore re-dispatched to other machines in the system when one or more AVRs lose their control capability. When increasing set-points, great caution needs to be taken due to that an excessive increase can result in a too high field current. Thus resulting in activation of the OEL and loss of voltage control. Increases should therefore preferably be performed in smaller steps at several generator instead of larger steps on fewer generators[14]. Reactive power control by means of voltage regulation which is explained above is discussed in several papers covering the topic and can for the interested reader be found in [32, 33].

2.4.3 FACTS devices

Installing flexible alternating current transmission systems (FACTS) devices in the power system has increased in parallel with the development of power electronics and the voltage range these can operate within. The use of FACTS devices gives the advantage of handling a power systems capability to control the flow of reactive power in a way which hasn't been possible before [17]. Being able to control the reactive power balance enables the PSO to control voltage stability and hopefully prevent and anticipate voltage collapse. The use of FACTS devices are

advantageous for mainly two approaches: to operate the power system in accordance with its power flow control capability; and to be able to improve the systems steady-state and transient stability [15, 17].

2.5 Simulation Models

In order to perform more realistic simulations of phenomena occurring in power systems, models are used to describe and characterize different parts of the system and how these respond to changes in dynamic simulations. Many of the models used in the simulations in this thesis were predefined in the Nordic32 test system. A number of models were however added to provide a more realistic view on voltage stability. Such models are presented below. The 3-bus case study also use several of the models stated in this section.

2.5.1 Essential models regarding voltage stability

When simulating voltage collapse, some models and their functions in the system have higher impact. Models for field current and OTLC were originally added to the Nordic32 test system but models for OEL, under voltage tripping of generators as well as distance relays had to be added. The following models are used in the simulations and are taken from [34].

SEXS

SEXS is a field current model which was already applied to the Nordic32 test system. It can be used for regulation of the field current for generators in PSS/E and thus also serves as an AVR. The voltage reference for the model can be changed to both increasing and decreasing the AVR set points and therefore be used to prevent voltage instability as described in Section 2.4.2.

MAXEX2

The model MAXEX2 was added to represent over excitation limiters in the simulations. It provides a three point characteristic current limit with corresponding time delays and uses the rated field current as base reference for the three current limits. It has a shorter activation timer for higher field current and vice versa for lower field current. When the OEL is activated it reduces the field current to 1.05

pu of rated field current. Adding a OEL model was important due to that it can have a significant effect on voltage stability due to the decrease in reactive power production as described in Section 2.1.5. When the MAXEX2 limiter model is applied, it reduces the field current below the lowest field current limit. A signal of whether the OEL is activated or not is also important for determining the systems margin to instability. The decrease in voltage caused by a OEL can result in activation of timers for under voltage tripping of generators.

VTGTPAT

Under voltage tripping of generators is a contributor to a voltage collapse due to that a systems becomes greatly weakened when a generator is tripped due to under voltage. The VTGTPAT model uses a over and under voltage threshold with a breaker timer and a breaker time delay. Thus tripping a generator a certain time after a generator voltage is below its threshold. VTGTPAT is a miscellaneous model which is applied to generators in the system.

OLTC1T

The OLTC1T is a two-winding transformer on load tap changer model which was originally added to several loads in the Nordic32 test system. It is used for transformers between lower voltage distribution areas and higher voltage transmission areas in the Nordic32 test system. The model is a branch model which is applied to branches which are equipped with transformers in PSS/E. The model uses a time delay for each tap changing operation between the detection of under/over voltage and tap change as well as a time constant for the tap changer.

2.5.2 Additional models

Several other models which were predefined in the Nordic32 system were also used. The models mainly represent generator and load characteristics which have an contribution to voltage collapse, but not in the same extent as the previously mentioned models. The models which are still important to notice can be seen in Table 2.1.

Table 2.1: Table over additional models used for the dynamic simulations of the Nordic32 test system.

Model	Description
GENCLS	The GENCLS model is a classic generator model which was only used in the two bus system to simulate an infinite bus. The model only have inertia and damping constants, which when set to zero in combination with a small generator reactance results in a infinite bus.
GENSAL	GENSAL is a generator model which was already applied to the Nordic32 test system. It describes the characteristics of a salient pole generator.
GENROU	GENROU is also a generator model which was originally applied to the Nordic32 test system. It describes the characteristics of a round or cylindrical rotor generator.
HYGOV	HYGOV is a governor model which was originally applied to the Nordic32 test system.
STAB2A	Stabilizer model applied to generators in Nordic32. Uses machine electric power as input. Output is used for SEXS field current model.
LDFRAL	LDFRAL is a load frequency model which was originally applied to all loads in the Nordic32 test system which causes the frequency to affect the constant current and constant power parts of the loads.
DISTR1	The DISTR1 model was used for 3 zone protection for branches in the Nordic32 test system. This was mainly for applying three phase faults to branches.

3

Evaluation of voltage stability indicators

This chapter contains three case studies which are performed to verify the theory behind the two indicators ISI and TPSI explained in Section 2.3.6 and their performance in different network setups. The three network setups investigated are a two-bus network, a three-bus network setup and the Nordic32 test system. The two-bus case study is designed to illustrate the behaviors of the indicators with an increasing load over time while the three-bus case study investigates the behaviors when a contingency occurs. The Nordic32 study contains two separate case studies designed to investigate the behavior of the indicators when a full voltage collapse occur.

3.1 Two-bus case study

The two-bus case study had the goal of verifying the voltage stability indicators and giving an understanding of how these perform. The simulations were performed on a simple two-bus system consisting of an infinite bus and a load bus. Due to it being only two buses, verification of the simulation results could easily be done. The simulations were performed using dynamic simulation in PSS/E which were automated by using Python scripts. The load was increased during the simulation at specified time steps up to the point of no converging solutions. A constant power factor was assumed and the voltage stability indicators were calculated for each level of load. The simulations were performed with and without switched shunt compensation at the load bus.

3.1.1 Network setup

The basic two-bus network used in the simulation can be seen in Fig. 3.1. The source bus is modeled as a swing bus while the load bus is modeled as a non-generating bus. The generator at the source bus was modeled with the dynamic model GENCLS. The system has a per-unit power reference of 100 MVA and a per-unit voltage reference of 132 kV. The load was increased with 1 MW for each simulation with a constant power factor of $\cos \phi=0.95$ and the branch between the buses is assumed to be lossless.

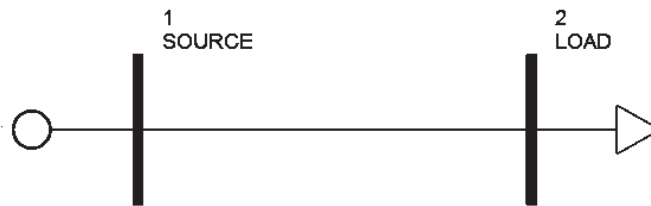


Fig. 3.1: The 2-bus network used in the simulation for verifying voltage indicators when no shunt compensation is active.

3.1.2 Indicator evaluation: Two-bus system, without switched shunt compensation

The behavior of the two indicators ISI and TPSI are investigated for the network setup explained in Section 3.1.1. Fig. 3.2 shows the performance of the voltage stability indicators as the system is getting closer to voltage collapse as the load is increased with time.

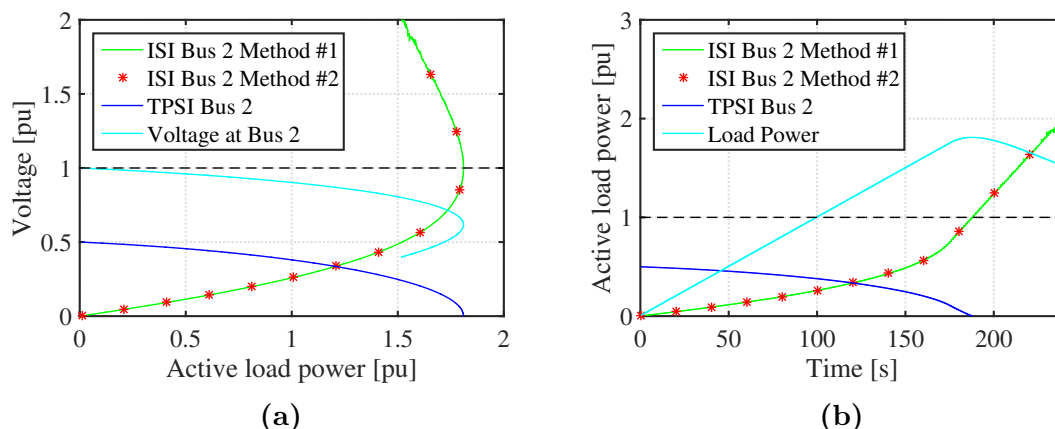


Fig. 3.2: Performance of the voltage stability indicators ISI and TPSI for a two bus system without compensation. **(a)** Voltage and voltage stability indicators as a function of the active power consumed by the load. **(b)** Active power consumed by the load and voltage stability indicators as a function of time.

Impedance stability index, ISI

The performances of the ISI using the two different methods as explained in Section 2.3.1 show similar result. Both methods reach the value of 1 at maximum power transfer. Looking at Fig. 3.2a where the quantities are plotted with the active power consumed by the load one can see the impact of the step wise increasing power. The voltage at the load bus is decreasing as a result of the increasing power which is voltage dependent. As the power increases the impedance that constitute the load decreases forcing the ISI to increase since it is getting closer to the thévenin impedance of the system.

Fig. 3.2b shows the same scenario but with time on the x-axis. This result is expected after what was said about Fig. 3.2a and the ISI reaches 1 after about 190 s which at the maximum power transfer occurs.

On the other hand, comparing the both methods of calculating the ISI show that the two methods are equivalent up to a certain point after maximum power transfer is reaches at time greater than 200 s. However, after this point no physical conclusions can be drawn since the lower part of the PV-curve only is used for theoretical explanation.

Transmission path stability index indicator, TPSI

The TPSI performs in accordance with theory and reaches zero at the point when maximum power transfer occurs. (2.18) describes the TPSI and as the voltage angle at bus 2 increases, making $V_R \cos \delta$ smaller, the TPSI decreases towards zero. When this happens the voltage drops over the line and over the load are equal which indicates instability. Both Fig. 3.2b and 3.2a show similar trends of the TPSI at bus 2 where it decreases with time/load power. The TPSI is only evaluated at bus 2 since it is the weakest bus of the two and there is only one path from the strongest bus to the weakest.

3.1.3 Indicator evaluation: Two-bus system, with switched shunt compensation

The behaviors of the indicators were also investigated when connecting a switched shunt compensation to the load bus. The compensation in MVar was set to a very large value to simulate a very efficient compensation scenario and to verify the indicators functionality even with high levels of compensation. The shunt compensation enables a higher maximum power transfer compared to the case without compensation and this is explained under Section 2.1.3.

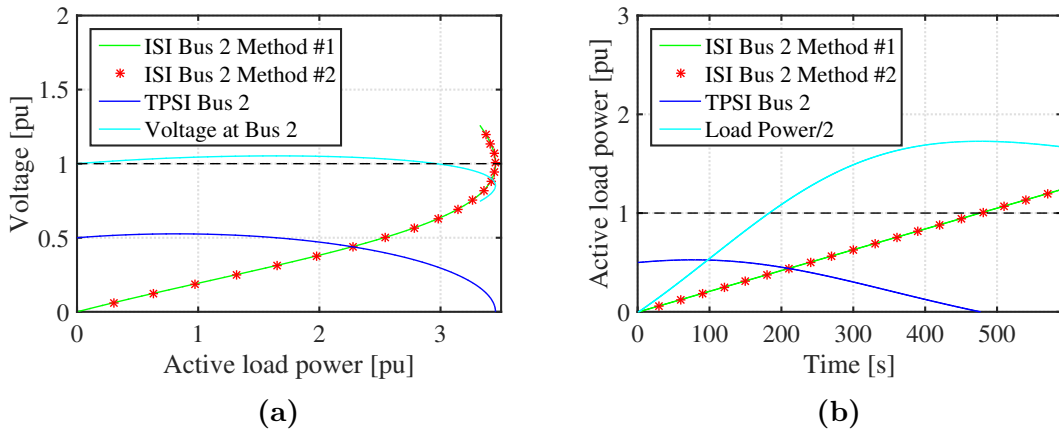


Fig. 3.3: Performance of the voltage stability indicators ISI and TPSI for a two bus system with compensation. (a) Voltage and voltage stability indicators as a function of the active power consumed by the load. (b) Active power consumed by the load and voltage stability indicators as a function of time.

The compensation at the load bus will force the voltage at the bus to increase

since the reactive power consumed by the load no longer is supplied through the line. This results in minimizing the voltage drop over the line.

Impedance stability index, ISI

The ISI-values in Fig. 3.3a and 3.3b increase more linear compared to the case without compensation which is a result of a more linear decreasing load impedance that has most of its reactive power provided directly from the shunt. The two methods of calculating the ISI give similar results. The critical point is reached at maximum power transfer, which is expected in accordance with theory. The compensation of reactive power increases the point of maximum power transfer compared to the case with no compensation, which result in that the system is operational for a longer period of time.

Transmission path stability index indicator, TPSI

The TPSI-values show the same trend as was shown with no compensation device. In Fig. 3.3b the TPSI seems somewhat flatter after 200 s compared to previous case and this has to do with the slowing increase of load power at this stage. The shunt device compensation at the load bus has a small impact on the voltage angle but has, on the other hand, a great impact on the voltage magnitude which has a theoretical connection to the compensation of reactive power.

3.1.4 Discussion

For the two bus system where the load is gradually increased both indicators perform in accordance with what previous work and theory have shown, both with and without compensation measures. Even though the two-bus network is stronger with compensation and is able to remain stable for a longer time and can at the same time transfer more power. The result is clear and it's possible to say that both indicators are able to indicate a voltage collapse for the type of network investigated in this section.

3.2 Three-bus case study

The three-bus case had the purpose of investigating how the voltage stability indicators responded to contingencies instead of a gradual load increase as was the

scenario for the two-bus case study. The three-bus case study was also used to evaluate the effect of different dynamic load model composition in PSS/E, as well as have the indicators behave under the impact of over excitation limiters. Be aware of that the intention of this section is not to cause a voltage collapse, it is the behavior of the indicators when a contingency occur and actions by the dynamic models that is investigated.

3.2.1 Network setup

A three-bus system with generators at bus 1 and 2 and loads at bus 2 and 3 as seen in Fig. 3.4 was investigated in this case study. Bus 3 served as the main bus for analyzing the indicators since it was the most exposed bus in terms of loading. In this case the complexity of the network is increased. Compared to the two bus case, a more complex admittance matrix used to estimate the thévenin impedance of the network was obtained and the impact of this could be examined. Being more complex, it also later made the transition to the Nordic 32 system less complicated. As effects could easier be evaluated in the three-bus system compared to Nordic 32.

The system has a per-unit power reference of 100 MVA and a per-unit voltage reference of 138 kV. The loads has a constant power factor of $\cos \phi=0.95$ and the branches between the buses are not loss less.

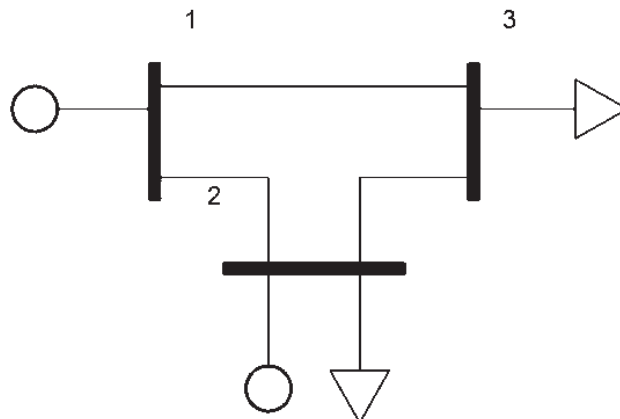


Fig. 3.4: The 3-bus network used in the simulation for verifying the TPSI and ISI.

The generators were modeled using the classical generator model GENCLS, sim-

plified excitation system model SEXS and the maximum excitation limiter model MAXEX2 which are described in Section 2.5 (see Appendix A.2 for model data). The excitation current limiter model was implemented to see how the effect of loosing voltage control at the generator terminal would effect the indicators. Expected results were to see a decrease in voltage as the limiter is activated, as well as an increase in the thévenin impedance as described in Section 2.1.5.

3.2.2 Indicator evaluation

The behavior of indicators were investigated as a line trip between bus one and three occurred. The simulations were preformed with the dynamic models mentioned in Section 3.2.1 to see the effects of usual dynamic scenarios in the power system. The result of the simulation can be seen in Fig.3.2.

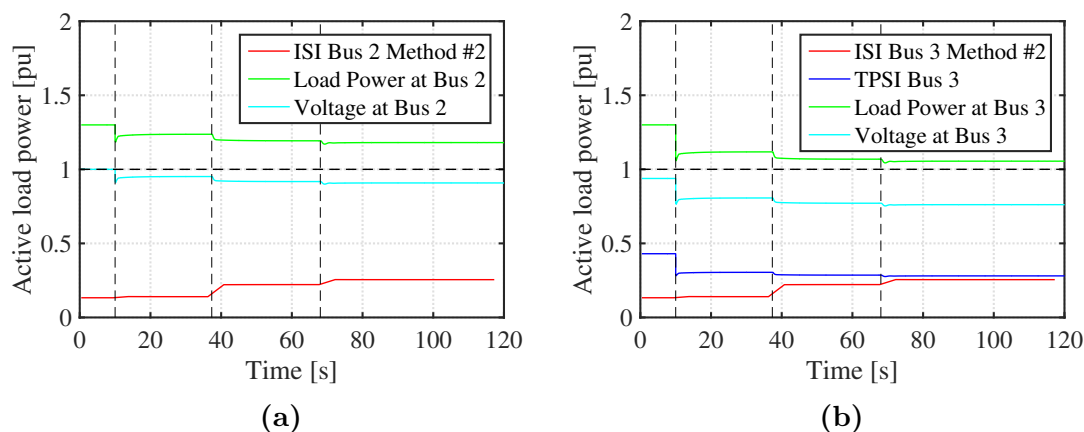


Fig. 3.5: Performance of the voltage stability indicators ISI and TPSI in the three bus case study. **(a)** Voltage and ISI indicator at bus 2 as a function of the time. **(b)** Voltage, ISI and TPSI at bus 3 as a function of the time.

At 10 s, the line between bus one and three was tripped, this increased the reactive power production at bus two in order to maintain the voltage level and supply the load at bus three with reactive power. However, this also increased the field current above the OEL for the generator at bus two, which was activated at 37 s. This was followed by an increase in field current for the generator at bus one as well, and the OEL for the generator is applied at 67 s.

Impedance stability index, ISI

In this case study and in the remaining report, only the ISI method 2 will be used. This was decided since method 1 which is based on consecutive measurements became too noisy during steady state operation (e.g if no immediate change of power flow between each step in time the estimate of the thévenin impedance will give a too small value and forcing the ISI value to infinity.). ISI method 2 gives for this reason a more uniform result without the use of consecutive measurements. As can be seen in Fig. 3.5, the ISI increases for both the tripping of line and activation of OELs. These trends can be seen both in Fig. 3.5a and 3.5b meaning that dynamic actions at one bus has an impact on the indicator values on adjacent buses.

The tripping of the line between bus one and three directly increases the thévenin impedance seen from bus three as can be seen in Fig. 3.6. It also decreases the load impedance because the load has a constant power characteristic. The decrease in load voltage thus decreases the load impedance according to

$$Z_{load} = \frac{V^2}{S^*} \quad (3.1)$$

The ISI at bus two is not heavily affected due to that the tripped line is not connected to it. The self-admittance and thus the thévenin impedance does not change as much as for bus three.

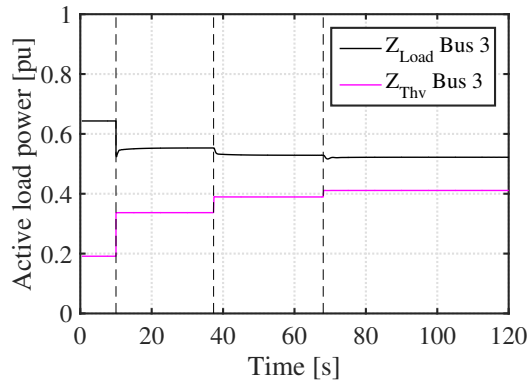


Fig. 3.6: Characteristics of the load impedance and the thévenin impedance at bus 3 as a function of time for the three bus case study.

The activation of OEL also increases the thévenin impedance due to that the

constant voltage is seen behind the generator reactance as discussed in Section 2.1.5. This further weakens the systems and the ISI increases. Due to less injected reactive power by the generators, the voltage is decreased and thus the load impedance.

Transmission path stability index indicator, TPSI

The TPSI is also affected by the system changes during the simulated case. The tripping of the line increased the voltage angle at bus three as well as it lowered the voltage at all buses. The voltage drop for the transmission path to bus 3 was therefore increased which gives an decreased TPSI value according to (2.20). The activation of the OELs mainly decreases the voltage levels which has less of an impact than an increase of voltage angle. The TPSI was only investigated for bus three as it was the weakest bus in the three bus system regarding voltage stability.

3.2.3 Discussion

The case study performed in this section have shown what effects line tripping and actions by dynamic models have on the ISI and TPSI indicators.

Method 1 used for estimating the thévenin impedance which was used to calculate the ISI did not give an accurate result for the ISI. This is explained by the small change in current in the denominator of (2.16) during steady state operation. The result is a unreasonably high value of the ISI. This result was also stated by V. Storvann which was discussed in Section 2.2. The second method was decided to be used to calculate the ISI in the remaining work for this thesis. Method 2 entails a higher reliability of the credibility of the indicator but it also demand a higher computational effort due to the need of updating the admittance matrix during each measurement point.

The indicators gave verdict in accordance with theory, the system gets weaker which the decrease and increase of the ISI and TPSI respectively show.

3.3 Nordic32 case study

This section contains two different base cases where contingency scenarios occur. For each case the designed scenarios lead to a full voltage collapse in the Nordic32

test system. The indicators were evaluated in both cases together with the voltage characteristics at the most critical buses. The base cases presented here contain the underlying sequence of events leading to a voltage collapse which is going to be prevented by implementing the system protection model which will be presented in next the chapter.

The Nordic32 test system has an increased complexity compared to the two and three-bus case studies. A greater number of buses introduces new challenges when implementing the calculations of the indicators. Further, the test system contains more dynamic models resulting in a more realistic simulation outcome of phenomena occurring in the power system.

3.3.1 Network setup

The Nordic32 test system is designed for simulation purposes of transient stability and long term dynamics. The test system is constructed for use in PSS/E [5]. The network seen in Fig. 3.7 is a 50 Hz grid consisting of a 400 kV main transmission system and some regional systems at 220 kV and 130 kV and is divided into 4 major parts:

- North: Consists of hydro generation and loads.
- Central: Consists of heavy loads and thermal power generation.
- Southwest: Consists of a few thermal generation units and loads.
- External: Consists of a mixture of generation and loads and are connected to the north.

Per-unit data is based on the voltage levels 130, 220 and 400 kV and a power base of 100 MVA and generation units have their own individual unit rating in MVA. Six dynamic models originally implemented in the test system are GENROU, GENSAL, SEXS, HYGOV and OLTC1 and their parameters can be found in the documentation of the Nordic32 [5]. DISTR1, MAXEX2 and VTGTPAT were added to this collection. All the models are further explained in Section 2.5 and settings can be found in Appendix A. The Nordic32 simulation model is closely related to the Nordic power network and contains many of its challenges. The challenges are associated with the high power production in the north and large loads in the south, resulting in a high power transfer from the northern part to the south. As a result of this, there are critical lines and buses which are vital for the system to operate at stable conditions. Such critical lines and weak buses are utilized in this chapter to create scenarios that lead to voltage collapse.

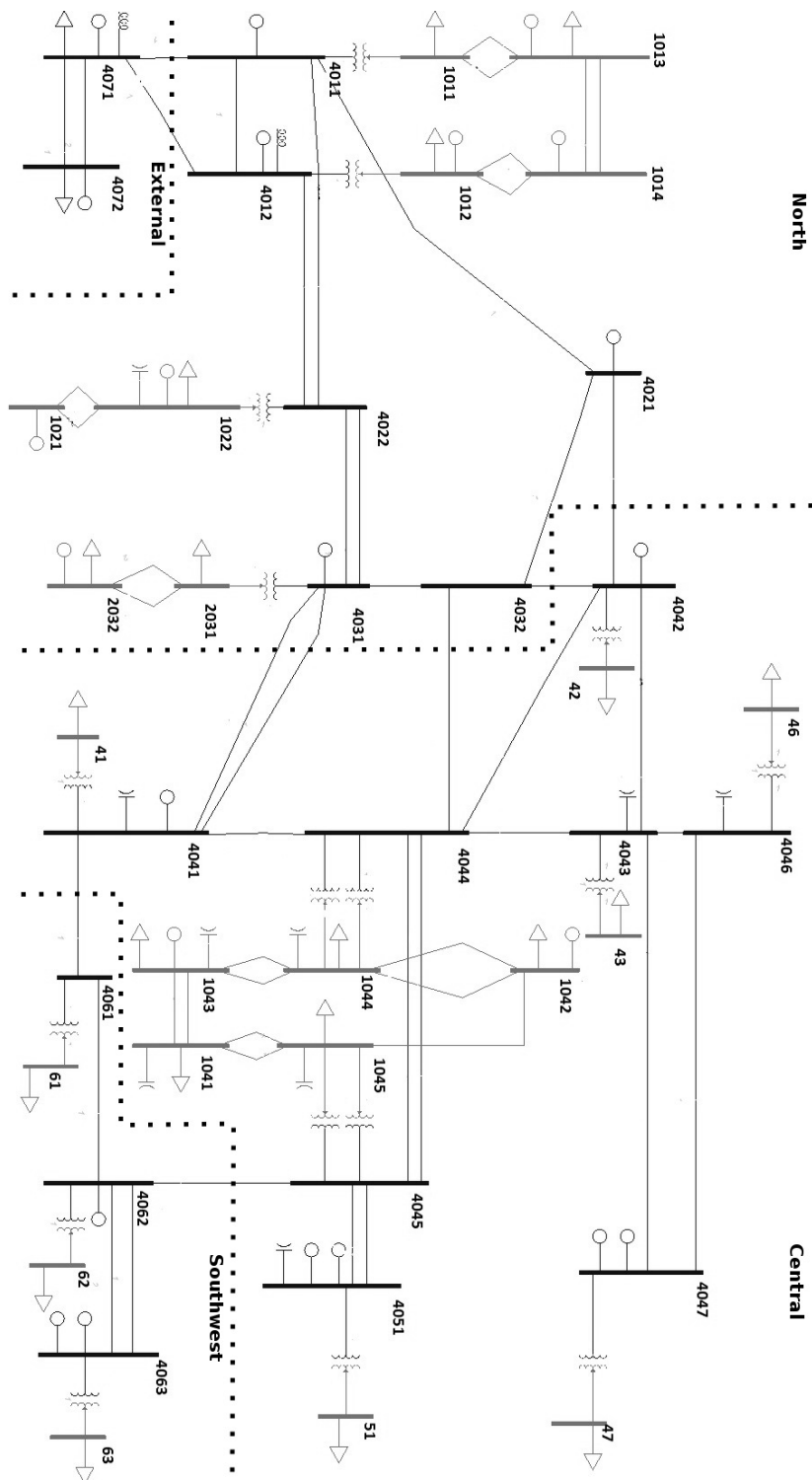


Fig. 3.7: The Nordic32 network which was used for verifying the implementation of the protection model.

3.3.2 Voltage instability cases

To evaluate the performance of the two voltage stability indicators in the Nordic32 test system measurement data was extracted from each of the two simulation cases and processed in Matlab in order to calculate the indicators. Two simulation cases with two different contingencies were performed. The scenarios used to cause the voltage collapse were designed in such a way that the system already was weakened due to modified load levels at some buses. This modification was done in order to force the system to a collapse. The simulation was run for 20 seconds and at this time a contingency occur, which leads to a weakened system. The weakened system leads to automatic actions of the dynamic models in terms of under voltage tripping of generators, activation of OELs, actions by distance relays and tap changing operations which in the end results in voltage instability and collapse. The dynamic models used to simulate each device in the Nordic32 test system are implemented with individual settings. However, the limit for under voltage tripping of all generators are set to 0.85 pu.

The goal of the simulations was to see how the indicators behaved to different changes in the system as well as to evaluate how much effort was needed to use these indicators in a more complex system. The cases presented in this section is further used in Chapter 4, together with the system protection model designed in this thesis. This in order to verify its functionality and ability to prevent a voltage collapse.

Case 1

The first case study was designed in such a way that distance relays was utilized which lead to a sequence of events that resulted in a voltage collapse for the modified Nordic32 test system. A three phase to ground fault was introduced at the line between bus 4032 - 4044 and the succeeding events can be seen in Tabel 3.1. The impact of these events can be seen in Fig. 3.8a which show the behavior of the two indicators and Fig. 3.8b show the voltage profiles at the buses 1042, 1043, 4042, and 4047 which were most affected by the contingency.

Table 3.1: Sequence of events leading to voltage collapse in the first case study of the Nordic32 test system.

Bus number	Event	Time [s]
4032 - 4044	Fault on line, tripped by distance relay	20.00
All transformer buses	OLTC actions	20.01-52.00
1043, 4031, 4042	OEL activated	48.00 - 53.00
1043	Under voltage tripping of generator	72.60
All transformer buses	OLTC actions	72.60 - 270.00
4047	OEL activated	104.00
1042	OEL activated	177.00
4042	Under voltage tripping of generator	270.00

The fault occurred at 20 s and after 2.5 simulation cycles (50 ms) the distance relay from bus 4032 to 4044 tripped the line. Between these two time instances the three phase fault gave rise to transient behavior of the voltage which decreased after the line was tripped and after which a somewhat more stable operating point was found. However, OLTC actions between 20.6 - 52 s lead to the activations of the OELs at the generator buses 1043, 4031 and 4042. The intention of the OLTC actions at this stage was to increase the voltage in the 130 kV grid, which is the weakest. An increase of this voltage will force the voltage in the 400 kV grid to decrease the flow of reactive power will change, leading to the OEL activation.

The TPSI and ISI behaved in the similar way as was shown in the two and three bus case studies. Bus 1041 was the weakest bus in the system, which is why the ISI was only evaluated for this bus. The activation of the OEL at bus 1043 at 52 s resulted in that the voltage at bus 1043 fell below the under voltage limit of 0.85 pu, and after a time delay of 20 s and a breaker time of 2.5 cycles the generator at 1043 was tripped at 72.6 s. The tripping gave rise to further OLTC actions and OEL activations at generator buses 4047 and 1042, at 104 and 177 s respectively, and the system was further weakened. Finally, at 270 s the generator at bus 4042 was tripped due to under voltage and the system collapses.

From Fig. 3.9 it can be seen that the collapse of the system has to do with voltage instability rather than frequency since the frequency recovers after the fault. The initial increase in frequency when the fault occurs is caused by the voltage drop over the loads. Due to the voltage dependency of the loads, there is a decrease in load power and therefore an increase in frequency. The primary governor reduces the frequency after this event. Other events such as activation of OELs and under

voltage tripping of generators also effect the voltage and therefore load power, will also affect the frequency and cause transients.

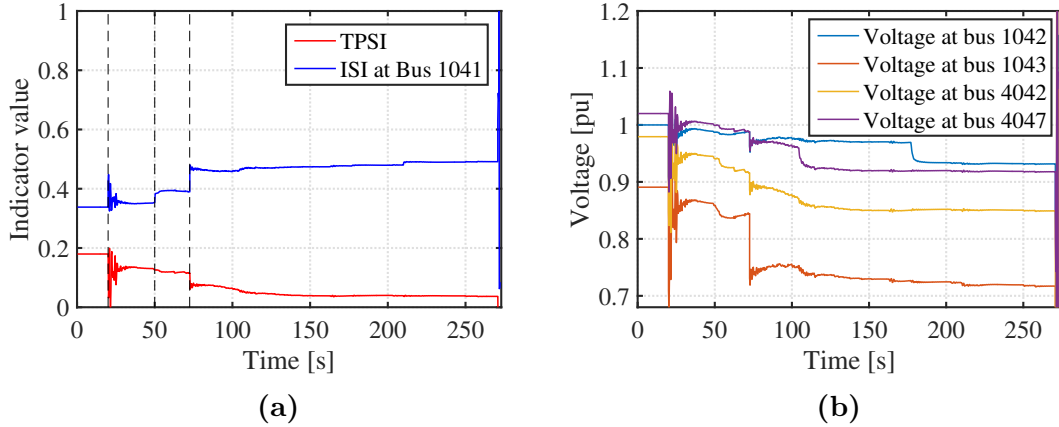


Fig. 3.8: Indicator values and voltage characteristics as a function of time of the first case study in the Nordic32 test system. (a) The characteristics of TPSI and ISI of the weakest bus for the first case study of the Nordic32 test system. (b) The voltage characteristics of the buses 1042, 1043, 4042 and 4047 which are most affected of the first case study of the Nordic32 test system.

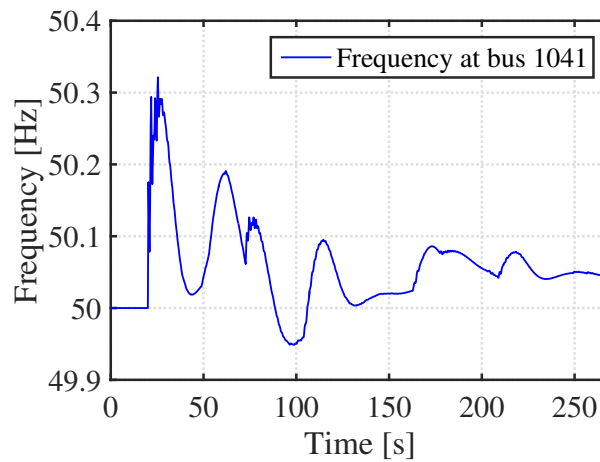


Fig. 3.9: Frequency characteristic at bus 1041 which is the weakest bus in Case 1. All buses do however show similar frequency characteristics.

Case 2

The second case study was designed as a scenario where the events in Table 3.2 lead to a voltage collapse after a initial loss of generation. The impact of these events on the indicator values can be seen in Fig. 3.10a and the voltage characteristics of buses 1043, 2032, 4041 and 4042 are shown in Fig. 3.10b. At 20 s the generator at bus 4042 was tripped. The events that followed were first activation of the OELs at buses 1022, 1043, 4031 between times 46.61 and 52.44 s. These events initiated OLTC actions at all transformers until 108 s, forcing the OELs at buses 2032, 4021 and 4041 to be activated one by one.

Table 3.2: Sequence of events leading to voltage collapse in the second case study of the Nordic32.

Bus number	Event	Time [s]
4042	Generator tripped	20.00
1022, 1043, 4031	OEL activated	46.61 - 52.44
All transformer buses	OLTC actions	46.61 - 108.00
2032, 4021, 4041	OELs activated	time >108.00
All transformer buses	OLTC actions	time >108.00
1043, 4021, 4041	Under voltage tripping of generators	131.00

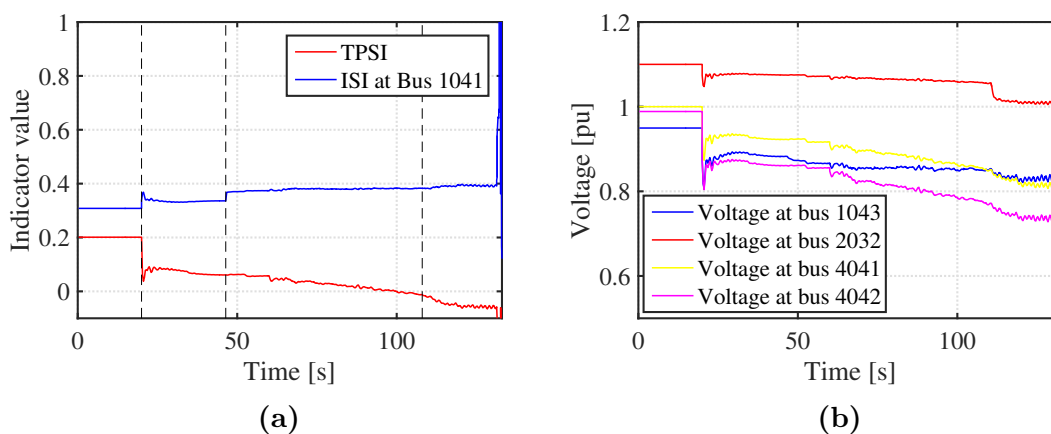


Fig. 3.10: Indicator values and voltage characteristics as a function of time of the second case study in the Nordic32 test system. (a) The characteristics of TPSI and ISI of the weakest bus for the second case study of the Nordic32 test system. (b) The voltage characteristics of the buses 1042, 1043, 4042 and 4047 which are most affected of the second case study of the Nordic32 test system.

The impact of the OELs does not show very clearly at times greater than 108 s, but the gradually decreasing voltage at this time was a result of this. OLTC actions together with the previous events at times less than 108 s result in that the generators at buses 1043, 4021 and 4041 are tripped due to under voltage which lead to a full system collapse.

The frequency in Fig. 3.11 show that the loss of the generator at bus 4042 causes a decrease in frequency. The system does however recover from this through the primary governors in the system. Other transients in the frequency can like the previous case be explained by that the load is voltage dependent. This can especially be seen towards the end of the simulations where activation of several OELs which decrease the voltage and therefore load power, thus an increase in frequency.

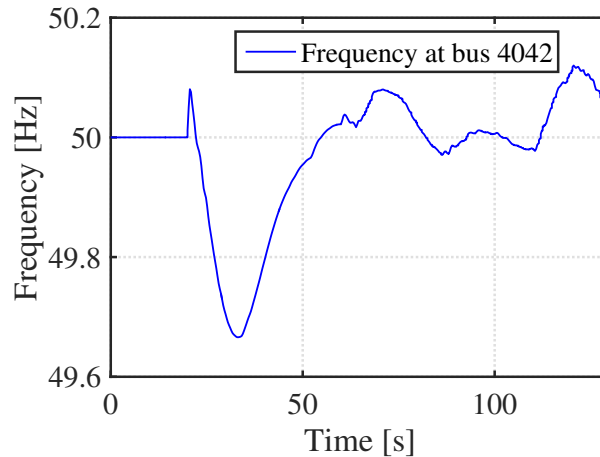


Fig. 3.11: Frequency characteristic at bus 4042 where 720 MVA of generation is lost in the beginning of the simulation.

3.3.3 Indicators evaluation

For each case presented in the previous section the behavior of the two indicators are investigated and evaluated in this section.

ISI

The ISI is for both cases only illustrated for bus 1041. The reason behind this is because this bus only had one load and a switched shunt connected to it, no gener-

ation occur which make 1041 the weakest bus in the network under the conditions for which the case is designed.

The initiating contingency causing the collapse show similar trends for both Case 1 and 2 in Fig. 3.8a and 3.10a respectively. The three phase fault in Case 1 created transients in the ISI which clearly can be addressed to the a voltage instability seen at this time instance in Fig. 3.8b. Overlooking the transients, an increase can be seen for the ISI for both cases just after the contingency takes place. Continuing with the sequence of events presented in Tables 3.1 and 3.2 for the two cases respectively, one can conclude that the ISI follows the characteristics connected to each contingency investigated until the collapse occur. Since the ISI is based on changes in the thévenin impedance of the system seen from the bus where it is calculated, the ISI tends to be more sensitive for events causing an impedance change compared to the TPSI. Looking at the ISI, OELs that are activated tend to be picked up and indicating a weakened system in greater extent than the effect OELs have on the TPSI.

TPSI

The TPSI algorithm is designed in such a way that it finds the path from the strongest bus to the weakest bus in the network. For the Nordic32 test system the strongest bus is often found in the northern part of the network and for the two case studies presented in this chapter the weakest bus was mainly 1041. After the initiating contingency for both cases the TPSI decreased with time as the events in Tables 3.1 and 3.2 for Case 1 and 2 respectively takes place. However, the TPSI compared to the ISI was in greater extent more prone to indicate a weakened system when events containing loss of generation occur. Since the calculations are dependent on voltage and its angle the impact of OELs was not as clear as for the ISI which can be illustrated at 52 s in Fig. 3.10a where the OEL of the generator at bus 4043 was activated. Another example of this phenomena can be seen when the OEL at bus 1042 was activated at 177 s. The voltage at bus 1042 in Fig. 3.8b illustrates this well. The ISI at bus 1041 indicated this event but the TPSI for the weakest path at this time instance does not indicate the activation of the OEL.

3.3.4 Discussion

The two case studies in Sections 3.3.2 and 3.3.2 showed an overall good performances of the TPSI and the ISI indicators. The indicators responded to the

dynamic events taking place in the system and are behaving in ways both theory and present two and three-bus case studies have shown.

The ISI have initial values close to 0.3 between 0 - 20 s in both cases which corresponds to the index value under current network conditions. This value only increases to about 0.5 just before the actual collapse of the system occur. This can be seen as a low indicator value just before collapse compared to 0.8 which often is chosen as alarm limit [4]. The reason for this low value is that the thévenin impedance of the system does not change significantly by the specific dynamic events taking place in Case 1 and 2. Since the ISI is based on the ratio between Z_{Thv} and Z_{Load} it tend to be more sensitive to change or loss of high impedance devices and loads in the system. The TPSI have initial values close to 0.2 between 0 - 20 s. The algorithm designed for calculating the TPSI in the Nordic32 test system is mainly based on the active power paths. There is a lot of active power transfer from the north and thus long active power paths with a large voltage angle difference. This assumption might not be true in other systems than the Nordic32. Based on the active power, the TPSI performs well for most dynamic events. OEL actions do not have the same clear impact as for the ISI but is still following the trends. On the other hand, the effect of OLTC operations have significantly higher effect on the TPSI compared to the ISI. This especially seen in Case 2 which is gradually weakened due to OEL activation and OLTC operations instead of under voltage tripping of generators or loss of transmission lines. In terms of computational times for the calculations the TPSI was much faster than the ISI which is one thing speaking against the ISI for further uses in this thesis. The time consuming calculation of the ISI had to do with the method used for calculating the ISI in this thesis.

For the system protection model described in the next chapter, only the TPSI was used as an indicator mainly due to the lower time consumption of the calculations as well as that the TPSI performed slightly better when indicating the stability margin compared to the ISI.

4

Prevention of voltage collapse

This chapter describes how the TPSI indicator was implemented in a PSS/E user defined model constituting the system protection model, and how it was used together with OEL and AVR signals to monitor and protect the system from voltage instability and collapse with help of a system protection scheme. The implementation of the model was verified and its performance was also evaluated.

4.1 The implementation of the system protection model

The purpose of the model was to monitor the voltage stability of the system in real-time as well as to be able to take corrective actions to mitigate instability and to prevent voltage collapse. The model was developed by implementing the indicator calculations from Chapter 3.3 continuously in the Fortran code. After this implementation the SPS by means of controlling synchronous generator AVR set-points and load shedding were implemented. The model was created as a user defined model within PSS/E and was defined as a miscellaneous model, as it was not supposed to be tied to a certain part or component in the system but as an external model monitoring the system as a whole. The model was written in Intel Visual Fortran 2005[35] as an .F90 file and compiled using the PSS/E Environment manager which links it to PSS/E libraries. The model was later called from the .dyr file in the simulation scripts written in Python.

4.2 Model working principle

The work flow of the model can be seen in Fig. 4.1 and the steps in this block diagram is performed at each time step. At each time step, synchronized measurements of voltage and angle are performed after which the TPSI are calculated. The system protection scheme uses two types of voltage instability mitigation actions. The first option, which is ranked as the first mitigating action in the SPS, is to increase AVR set-points with a predefined percentage for generators in the network. The second one is load shedding, which is performed if the increase of the AVR set-points is not enough as mitigating action. The increase of AVR set-points are triggered by reduction in a reactive power production from synchronous generators caused by OEL activation and therefore use this signal. This action attempt to balance out the loss of reactive power production. The triggering event for the model to start shed loads is based on the value of the TPSI.

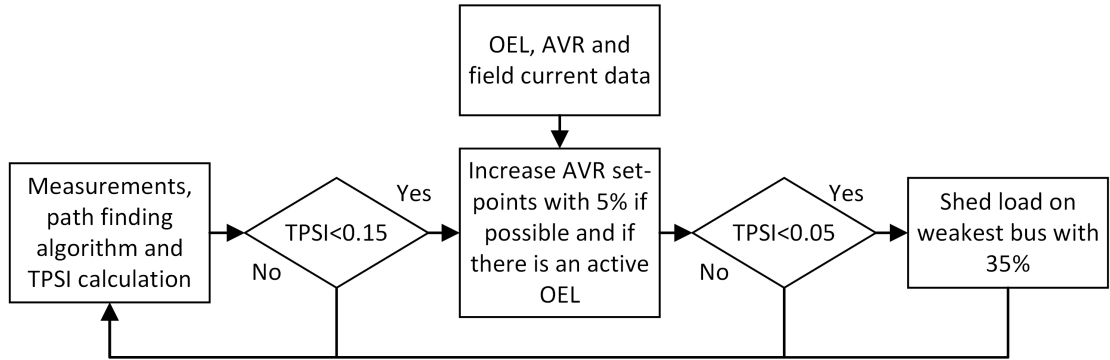


Fig. 4.1: Block diagram of the system protection model which is run at each simulation time step in PSS/E

4.3 Settings of the model

The load shedding criterion was set to when the TPSI reached a value below 0.05, which in this thesis was decided to be the limit for when the margin to instability is critically low. The choice of limit for load shedding was based on consecutive simulation results which showed that the risk for under voltage tripping of generators increased for TPSI values lower than 0.05. For the simulations presented in this chapter, loads were shedded by 35% and the reason behind this is explained later in this chapter. The criterion for increasing AVR set-points were set so that the TPSI needed to be set lower than 0.15 and the increase will occur when the first OEL is activated to compensate for the loss of reactive power.

The percentage of how much to increase the AVR set-point and how much load to shed, as well as the TPSI threshold for load shedding are changeable settings in the dynamic data file from where PSS/E calls dynamic models (Appendix B).

4.4 Verification of the model

To verify the model, the result of the calculation of the TPSI which were calculated using Matlab in Chapter 3.3 was compared to the TPSI which was calculated by the system protection model. The same base cases that was analyzed using Matlab in the previous chapter were again used for this verification. Extracting the TPSI values from the model was done by assigning it an output channel in PSS/E from which the values were extracted and plotted in Matlab. The TPSI calculated by the model in real-time proved to be identical to the one calculated in Matlab which is illustrated in Fig. 4.2 for both Case 1 and 2.

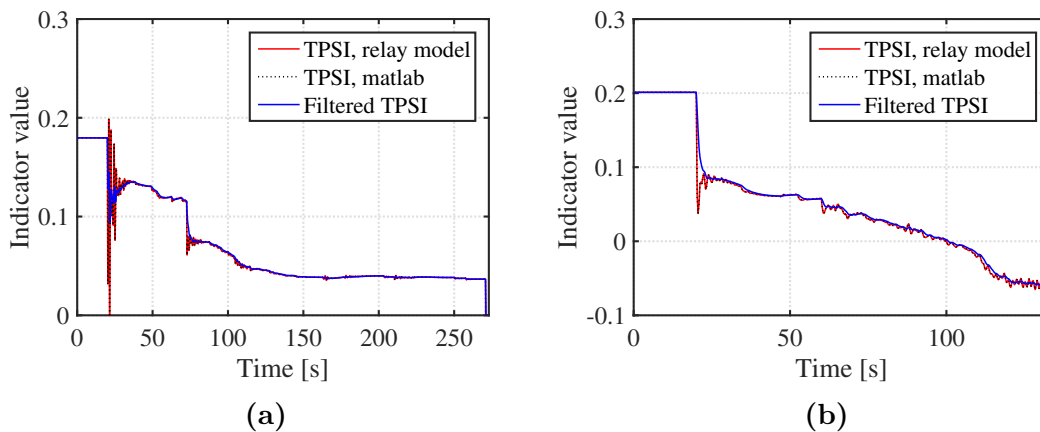


Fig. 4.2: A comparison between calculating the TPSI with Matlab and with the system protection model as well as the filtered signal of the TPSI. TPSI calculated by both Matlab and the system protection model as well as a filtered TPSI signal for Case 1 in (a). TPSI calculated by both Matlab and the system protection model as well as a filtered TPSI signal for Case 2 in (b).

In addition to the original TPSI signal a first order low pass filter was implemented to filter out the effects of transients on the TPSI value from the model. In this way the TPSI becomes more reliable for determining the systems margin to instability. The filtered TPSI-values were delayed with one time step due to the model structure in PSS/E and how models are executed and called for in the software.

4.5 Evaluation of the system protection model

The system protection model is designed to prevent voltage instability in two steps, the first step is to increase the AVR set-points for generators capable of increasing reactive power output without the risk of entering the limit of over voltage at the bus. Furthermore, an increase of the AVR set-points is not performed at generators where the OELs are active, nor for generators with field currents above their rated value. If the first step is not sufficient for preventing a voltage collapse the model will shed load at the bus with the lowest TPSI. The functionality of the model is evaluated by observing how well the model prevents the voltage collapse occurring in the two base cases presented in Section 3.3.2.

4.5.1 Case 1

Starting with the least severe, Case 1, which had a longer time after the fault until the system collapsed. Rerunning the simulation of the same case presented in Section 3.3.2 but this time with the system protection model implemented. The result can be seen in Fig. 4.3b. This clearly show that the model prevents the voltage collapse which previously occurred at approximately 270 seconds. With the corrective actions in the SPS the TPSI value was finally stabilized at around 0.09. Bus voltages were stabilized to values slightly lower than before the fault, which can be seen in Fig. 4.3b.

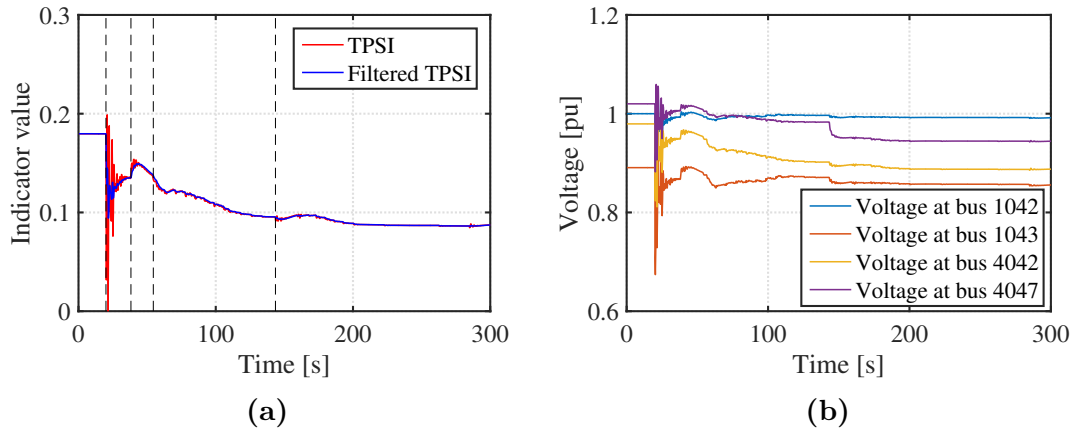


Fig. 4.3: Case 1 TPSI in (a) and bus voltages in (b) for critical buses after the fault with corrective actions through AVR set-point increase performed by the system protection model resulting in a prevention of voltage collapse.

Due to that there is no major simulation events after 200 seconds the system can be considered to have reached a new steady state. After this point, no OEL timers are activated as well as only a few OLTC operations. The TPSI threshold for load shedding was 0.05 for this simulation, although it can clearly be seen that TPSI never reaches this value. The increase of AVR set-points is initiated when the TPSI is below 0.15 and when an OEL is activated.

The simulation scenario of Case 1 with the system protection model implemented followed a sequence of events which can be seen in Table 4.1. The AVR set-points are increased with 5% for a number of selected buses when then first OEL at bus 1022 is activated after 38 seconds, where the effect on bus voltage and reactive power production at buses 1022 and 4021 can be seen in Fig. 4.4. The increase resulted in that the two generators at bus 4047 which in Section 3.3.2 tripped due to under voltage remained in operation due to the increased bus voltage at 4047 and now only experienced activation of its OEL at 143 seconds. The system experienced an activation of a number of OELs which forces the OEL at the generator at bus 4062 to activate at 158 seconds which previously had its AVR set-point increased at 38 s. This is due to a decrease of reactive power production of the other generators.

Table 4.1: Sequence of events for Case 1 with the system protection model

Bus number	Event	Time [s]
4032 - 4044	Fault on line, tripped by distance relay	20
1022	OEL activated	38
4011, 4012, 4021, 4041, 4051, 4062, 4063	AVR set-point increased with 5%	38
4031	OEL activated	53
4042, 1042	OEL activated	56 - 58
All transformer buses	OLTC actions	60 - 170
4047	OEL activated	143
4062	OEL activated	158

The bus voltage at bus 1043 for the new steady state after 200 s were only 0.87 pu making the generator prone to a under voltage trip if additional faults would occur. This is however to be compared with the base case in Section 3.3.2, where the generator at 1043 was tripped due to under voltage 50 seconds after the fault. The system is operating in a weakened state and more mitigating actions could

possibly be performed to increase the margin to instability. The immediate collapse is however prevented due to the increase of AVR set-points and no load shedding was needed for this case.

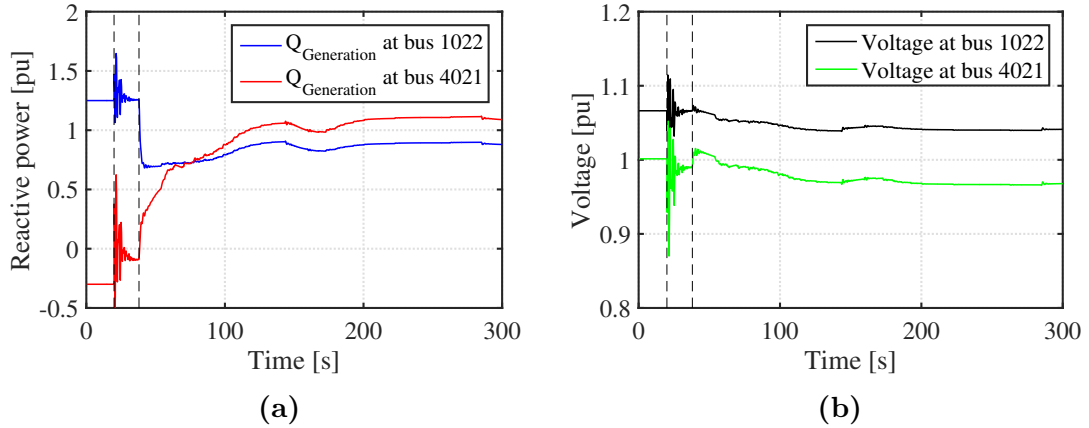


Fig. 4.4: Reactive power production in (a) and voltages in (b) for bus 1022 which generator experienced activation of OEL and therefore initiated the AVR set-points increase and for bus 4021 which is one of the buses with increased AVR set-points

4.5.2 Case 2

Case 2 which was initialized by a tripped generator at bus 4042 was more severe with a shorter time course until collapse compared to Case 1. For this case, an increase of AVR set-points did not prove to be enough to prevent the collapse and load shedding had to be utilized. After this action the system margin to voltage instability was increased and when the system had stabilized it had a TPSI value at around 0.09 which can be seen in Fig. 4.5a. The full sequence of events can be seen in Table 4.2. The voltages for the more exposed buses of the network are kept at lower level compared to before the fault which can be seen in Fig. 4.5b. This is mostly due to the loss of reactive power production at bus 4042 where the generator is tripped. This bus is a critical part of the network and can be seen as a node where a high power transfer from the northern area to the southern and central area of the Nordic32 takes place.

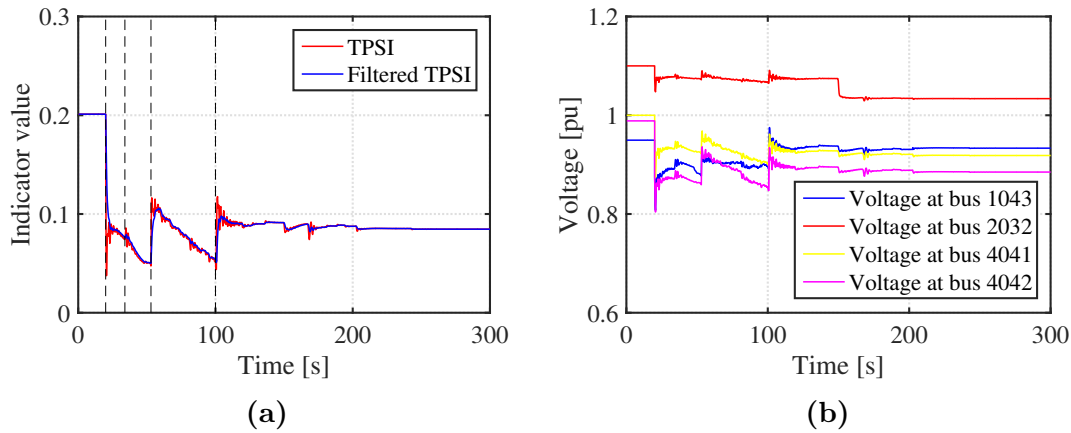


Fig. 4.5: Case 2 TPSI in (a) and bus voltages in (b) for critical buses after the fault with corrective actions through AVR set-point increase performed by the system protection model resulting in a prevention of voltage collapse.

Table 4.2: Sequence of events for Case 2 with the system protection relay model

Bus number	Event	Time [s]
4042	Generator tripped, 630 MW 350 MVA	20
1022	OEL activated	34
4011, 4012, 4051, 4063	AVR set-point increased by 5%	34
4031	OEL activated	52
42	Load shed by 35 % 172 MVA	53
4021	AVR set-point increased by 5%	55
All transformer buses	OLTC actions	time >60
4047	OELs activated	81
46	Load shed by 35 % 254 MVA	100
2032, 4011	OELs activated	150 - 166

The increase by 5 % of the AVR set-point when the first OEL is activated at bus 1022 after 34 seconds was not enough to save the system and had to be supplemented by load sheds of 35 % at bus 42 and 46 after 53 and 100 seconds, until the systems stability margin can be maintained. The shedding occurs at two different buses due to that the weakest bus according to the TPSI is changed after the first load shed, where the effect on voltage and apparent power for these

buses can be seen in Fig. 4.6. The percentage value to shed loads with was based on consecutive simulations where different percentages were tested and evaluated. A too low percentage increased the number of times loads had to be shed to avoid a collapse. As well as that a low percentage in the end resulted in a higher accumulated load shed. A high percentage could efficiently prevent instability and collapse, however, this also resulted in an extensive amount of load shed at only one bus. If load shedding instead occurs at a couple of buses in the system when needed, then the improvement of the overall system stability proved to be better. For this reason 35% was found to be a balanced amount due to that the load shedding was divided between two buses as well as that the total amount of load shed was kept at a low level compared to the overall load of the system. When and where the load shedding occurs are entirely based on the value of the TPSI.

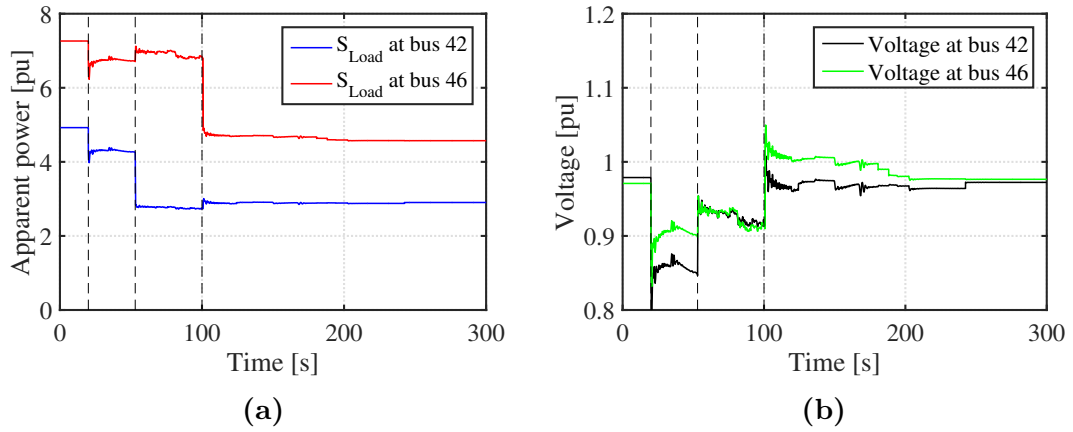


Fig. 4.6: Apparent load power in (a) and bus voltages in (b) for bus 42 and 46 which experience load shedding at 53 and 100 seconds respectively.

Further increasing the AVR set-point could result in a over voltage at certain buses in the northern part of the network and could instead resulted in negative results. The activation of OELs at 52 and 81 s for generators at buses 4031 and 4047 respectively cause a major loss of reactive power production resulting in a loss of voltage control. Since these generators stand for the major reactive power production in the transfer area, the generator at bus 4011 also reaches its field current limit resulting in OEL activation at 166 seconds. The collapse is prevented through the increase of AVR set-points together with the shedding of load at the two occasions. One can however argue that the load shedding is at a minimal level due to that OELs are still active when system enter its new steady state. It is also important to mention that minimal shedding of load is desired due to that the main purpose of a power system is to supply power to the customers. In other

words, load shedding can be seen as a last resort for maintaining system stability. In addition to this, the total load shed did not equal the generation lost by tripping of the generator at bus 4042. This can be explained by that other generators have increased power production as well as because of the load's voltage dependency and thus reduced load power. It is also worth to note that the system frequency was slightly lower than 50 Hz when the system was stabilized.

4.6 Discussion

The system protection model designed in this thesis has proved its ability to prevent a voltage collapse in the two cases investigated in this chapter. The first case responded well to an increase of the AVR set-point and the second case to load shedding. The immediate effect of an increasing AVR set-point was that it could prevent under voltage tripping of generators, thus maintaining a higher generation of power to supply the grid. Since the shunt compensation in the Nordic32 test system is fixed with the reactive production proportional to the square of the voltage, an increase in voltage at buses with shunt compensation further strengthens the effect of increasing the AVR set-points. However, the set-point increase has to be done carefully in order for the increase not result in a over voltage for buses with already high voltage in areas with high power production. Further, a to large increase of the set-point of a generator could increase the field current above the field current limit, especially if nearby generators experiences activation of their OELs.

The load shedding is an effective method to restore stability and for increasing the margin to instability. It is however important to note that it is used mainly as the last option as well as keeping the load shedding at a minimal amount. It is also worth to note that these actions are short term and used in emergency situations.

While indicators such as the TPSI and the ISI can be used to determine the margin to voltage stability, it is important to add that stability indicators do not show all weaknesses in a system. Other important signals to consider are for example signals from OELs, timers for under voltage tripping, OLTC actions etc. which have to be used in combination with voltage stability indicators in order to monitor all events in a network. A combination of multiple stability indicators and input signals mentioned above will help to increase the credibility of a system protection model and make it more robust. As an example, in case of an under voltage trip, a system can quickly become significantly weakened and experience instability at buses if more indicators are utilized indicating the same event the probability to take the

right mitigating actions are increased. This is however a balance, since using a model with many inputs requires a complex solution with longer computational times.

For the system protection model in PSS/E, measurements for the TPSI could easily be performed due to that voltage and angle are synchronized for each time step. To perform synchronized measurements can however be a challenging task in a real system where communications can be a limiting factor.

5

Conclusions and future work

5.1 Conclusions

This thesis was focused on developing a system protection model and evaluating how such model can use voltage stability indicators together with signals from OELs as inputs in order to monitor the voltage stability of the system. Depending on the value of the two input signals the model will initialize and utilize SPSs to prevent a voltage collapse. The model described in the previous chapter was successfully developed and implemented in PSS/E. The conclusions of the results of the present work leading up to a functional system protection model is presented below.

- The indicators which were decided to be used in this thesis were the ISI and the TPSI. This decision was based on the advantages and disadvantages of the six different voltage stability indicators discussed in [4].
- It was shown that the ISI gave the best result when calculated by means of estimating the thévenin impedance with help of the system admittance matrix rather than by estimating it with consecutive measurements of bus voltage and current. Consecutive measurement resulted in a noisy ISI signal.
- Both the ISI and the TPSI behaved as expected to a line trip leading to a sequence of dynamic events amongst activations of OELs.
- Implementing and evaluating the behavior of the two indicators in the Nordic32 test system did however show that the ISI was not suitable for use in the system protection model. This conclusion was drawn because of the need of a large amount of computational power resulting in long calculation times

compared to the TPSI. In parallel with this, the ISI was not as accurate as the TPSI in indicating the margin to voltage collapse.

- The system protection model was developed and implemented in PSS/E with the TPSI and OEL signals as inputs. The model was designed to initialize a SPS consisting of increasing AVR set-points of generators if an OEL is activated at the same time as the value of the TPSI is below 0.15 and to shed load when the TPSI fell below 0.05.
- The calculation of the TPSI done in the model was verified by comparing it with external calculations performed in Matlab and these showed the same result.
- Two base cases leading to a voltage collapse was designed for the Nordic32. The model and associated SPS successfully prevented the voltage collapse in both cases, for the first case a increase of AVR set-points was enough to prevent voltage collapse and in the second case both increase of AVR set-point and load shedding was utilized to save the system from collapse.

5.2 Future work

There are several ways to continue and optimize the work done in this thesis. Suggestions on such work are presented below, starting with the voltage stability indicators.

- Future work can be done concerning the ISI and how to estimate the thévenin impedance in the most efficient and accurate way as this is the greatest challenge concerning this indicator. The two methods presented in Section 2.3.1 can both be investigated further. Method 1 for estimating the thévenin impedance needs an algorithm to separate indicator values for which the change between consecutive measurements are too small. Designing such algorithm could in best case result in that Method 2 for calculating the ISI, which was used in this thesis, could be abandoned to advantages of Method 1 which requires less computational power. If this is achievable, optimizing Method 2 in terms of decreasing the time of calculation could be done.
- Regarding improvement for the TPSI, it could be utilized to find several weak buses with low TPSI values without increasing the computational time as the path finding algorithm in its current form supports this. This could for example give more options regarding load shedding, for example when concerning prioritized loads. Optimization to decrease the computational

time could also be performed, although this could disable the possibility to find multiple weak buses. Further development of TPSI can therefore be directed to how it will be used for decision making.

- The model developed in this thesis was only designed for use with the Nordic32 test system. Depending on the limitations regarding which information that is available in PSS/E when developing a user defined model, it would be interesting to see a generic system protection model.

Continuing with the system protection scheme. The protection scheme was designed with two mitigating actions, increase of AVR set-points and load shedding. Further improvements of how these mitigating actions are implemented in the model are proposed here:

- First of all could the algorithm deciding what actions to take be extended with combinatorial optimization of load shedding [30]. And if no other option than to shed load remains, the shedding in a certain area of the network should be performed according to a predetermined order where the least prioritized load is shedded first. In other words, improve how the algorithm handles and evaluates the three factors, when, where and how much preventive actions to take.
- Another interesting topic which can be improved is how to increase (or decrease) the AVR set-points in an optimal way. This due to that this corrective action can have a significant effect when preventing voltage collapse. The AVR set-points could continuously be adjusted to re-dispatch production of reactive power, and done so in a optimal way so that activation of OELs are prevented. The challenging part could be that the limitations of each generator have to be considered individually as well as how they interact with each other.
- Additional corrective action can also be implemented and this would probably require a more complex algorithm to decide what actions to take and when. Such corrective actions could be blocking of zone 3 distance relays, blocking of OLTC or through adding FACTS models to the simulation. To be noted however, a more complex system protection model may lead to more time consuming simulations.

References

- [1] I. Adebayo, et al., *A comparison of voltage collapse point prediction capabilities of voltage stability index and inherent structural characteristics*, AFRICON (2015) 1–5.
- [2] C. Subramani, et al., "Stability Index Based Voltage Collapse Prediction and Contingency Analysis", in *Journal of Electrical Engineering and Technology* 4 (4) (2009) 438–442.
- [3] I. Dobson, et al., "Voltage collapse in power systems", in *IEEE Transactions on power systems* (1992) 40–45.
- [4] V. Storvann, *Maintaining voltage stability, An Analysis of Voltage Stability Indicators and Mitigating Actions*, diploma thesis, NTNU, Trondheim (06 2012).
- [5] K. Walve, *A Cigré test system for simulation of transient stability and long term dynamics*, Svenska Kraftnät, 1993.
- [6] *PSS®E 34 Program Operation Manual (POM)*, Siemens Power Technologies International, March 2015.
- [7] Python Software Foundation, *Python web page*, <https://www.python.org/> (2016 (accessed May 24, 2016)).
- [8] Tobias Burnus, *GFortran Standards*, <https://gcc.gnu.org/wiki/GFortranStandards> (2016 (accessed May 24, 2016)).
- [9] MathWorks, *Matlab web page*, <http://se.mathworks.com/> (2016 (accessed May 24, 2016)).
- [10] W. Pimjaipong, et al., "Blackout prevention plan - The stability, reliability and security enhancement in Thailand power grid", in *IEEE Transmission and distribution conference and exhibition: Asia and pacific* (2005) 1–6.

- [11] E. A. Dyrstad, *Relay lab at NTNU*, diploma thesis, NTNU, Trondheim (06 2014).
- [12] G. Andersson, et al., "Causes of the 2003 Major Grid Blackouts in North America and Europe, and recommended means to improve system dynamic performance", in *IEEE Transactions of power systems* 20 (4) (2005) 1922 – 1928.
- [13] A. Chakrabarti, et al, *An Introduction to Reactive Power Control and Voltage Stability in Power Transmission Systems*, PHI Learning Private Limited, New Delhi, 2010.
- [14] V. Cutsem, C. Vournas, *Voltage stability of electric power systems*, Springer Science+Business Media, Dordrecht, 1998.
- [15] P. Kundur, *Power System Stability and Control*, McGraw-Hill Inc, 1994.
- [16] H. Saadat, *Power system analysis*, PSA Publishing, 2010.
- [17] J.Hossain, H. Pota, *Robust Control for Grid Voltage Stability: High Penetration of Renewable Energy*, Springer, 2014.
- [18] M. Glavic, *Power system voltage stability: a short tutorial*, University of Liège, Belgium, <http://www.montefiore.ulg.ac.be/~glavic/REE-Seminar.pdf> (2016 (accessed April 26, 2016)).
- [19] C.Canizares, et al, "Voltage Stability Assessment: Concepts, Practices and Tools", in *IEEE Power and Energy Society*.
- [20] M.Begovic, et al, "A novel method for voltage instability protection", in *Proceedings of the 35th Hawaii International Conference on System Sciences* (2002) 802 – 811.
- [21] K.Vu, et al, "Use of Local Measurements to Estimate Voltage-Stability Margin", in *IEEE Transactions of power systems* 14 (3) (1999) 1029 – 1035.
- [22] L. Warland, *A Voltage Instability Predictor Using Local Area Measurements*, P.hd thesis, NTNU, Trondheim (02 2002).
- [23] D. Duong, K. Uhlen, "Online Voltage Stability Monitoring Based on PMU Measurements and System Topology", in *IEEE International Conference on Electric Power and Energy Conversion Systems, Turkey* (2013) 1–6.
- [24] F.Gubina, B.Strmcnik, "Voltage collapse proximity index determination using voltage phasors approach", in *IEEE Transactions on Power Systems* 10 (2) (1995) 788–794.

-
- [25] M. Sniedovich, "Dijkstra's algorithm revisited: the dynamic programming connexion", *Control and Cybernetics* 35 (3) (2006) 599 – 620.
- [26] G. Verbic, Gubina.F, "A novel concept for voltage collapse protection based on local phasors", in *Transmission and Distribution Conference and Exhibition 2002: Asia Pacific. IEEE/PES 1* (2002) 124 – 129.
- [27] Musirin.I, Rahman.T.K.A, "Novel fast voltage stability index (FVSI) for voltage stability analysis in power transmission system", in *IEEE, Research and Development, 2002. SCORed 2002. Student Conference on* (2002) 265 – 268.
- [28] Ramirez-Perodomo.L, Lozano.A, "Evaluation of indices for voltage stability monitoring using PMU measurements", in *INGENIERÍA E INVERSIÓN* 34 (3) (2014) 44 – 49.
- [29] City of Cape town, *Load shedding explained*, <https://www.capetown.gov.za/en/electricity/Pages/Loadshedding-explained.aspx> (2016 (accessed May 2, 2016)).
- [30] T. Cutsem, C. Moors, D. Lefebvre, "Design of load shedding schemes against voltage instability using combinatorial optimization", *Power Engineering Society Winter Meeting, 2002. IEEE 2* (2002) 848 – 852.
- [31] A. T. Le, et al., "A Combined Zone-3 Relay Blocking and Sensitivity-Based Load Shedding for Voltage Collapse Prevention", *2010 IEEE PES Innovative Smart Grid Technologies Conference Europe (ISGT Europe)* (2010) 1 – 8.
- [32] J. L. Agüero, et al., "Interaction between AVR reactive power control and high power ac-dc Converter Control as possible cause of instability", in *2012 IEEE Power and Energy Society General Meeting* (2012) 1 – 7.
- [33] O. H. Abdalla, et al., "Voltage and reactive power control in Oman transmission system", in *Power Engineering and Optimization Conference (PEOCO), 2013 IEEE 7th International* (2013) 495 – 500.
- [34] *PSS®E 34 Model Library*, Siemens Power Technologies International, March 2015.
- [35] Intel, *Intel Fortran web page*, <https://software.intel.com/en-us/fortran-compilers> (2016 (accessed May 25, 2016)).

A

Simulation model data

A.1 Two-bus case study

A.1.1 Generator data

Table A1: Generator data used in the simulation for the two bus case study, dynamic data from .dyr file.

Generator source impedance (pu)	0.000001
GENCLS dynamic model	'GENCLS' 1 0 0/

A.1.2 Branch data

Table A2: Branch data used in the simulation for the two bus case study

Line R (pu)	0.0
Line X (pu)	0.20
Charging B (pu)	0.0

A.1.3 Load data

Table A3: Load data used in the simulation for the two bus case study, a constant power factor of $\cos \phi=0.95$ was used.

Initial active power (MW)	1.0
Initial reactive power (MVA_r)	1.0
Load increment (MW) per time step	1.0

A.1.4 Switched shunt data

Table A4: Switched shunt data used in the simulation for the two bus case study

Block 1 steps	500(Mvar)
Block 2 steps	-500 (Mvar)

A.2 Three-bus case study

A.2.1 Generator data

Table A5: Generator data used for both generators in the simulation for the three bus case study, dynamic data from .dvr file.

Generator source imp. (pu)	0.2
Generator power base (MVA)	100
GENSAL dynamic model	'GENSAL' 1 5 .05 .1 3 0 1.1 .7 .25 .2 .15 .1 .3/
SEXS dynamic model	'SEXS' 1 .2 20 50 .1 0 5/
MAXEX dynamic model	'MAXEX2' 1 1 1.7 1.1 30 1.22 10 1.75 2 1.05 1 -0.05/

A.2.2 Branch data

Table A6: Branch data used for all three branches in the simulation for the three bus case study.

Line R (pu)	0.001
Line X (pu)	0.20
Charging B (pu)	0.0

A.2.3 Load data

Table A7: Load data used for both loads in the simulation for the three bus case study.

Active power (MW)	130.0
Reactive power (MVar)	42,7346

A.3 Nordic32 case studies

A.3.1 Case 1 data

Table A8: Modified load data used for Case 1 in the Nordic32, remaining buses have original load levels.

Load	Active power P (MW)	Reactive power Q (MVar)
42	450	200
1041	900	350
1042	400	250
1043	300	150
1044	600	300

A.3.2 Case 2 data

Table A9: Modified load data used for Case 2 in the Nordic32, remaining buses have original load levels.

Load	Active power P (MW)	Reactive power Q (MVar)
41	550	200
42	450	200
47	200	100
61	500	200
1041	600	300
1042	300	150
1043	300	150
1044	900	400

A.3.3 DISTR1 Mho settings used in the Nordic32

The settings for the DISTR1 model can be found in the Table A10 on the next page and the settings for the other dynamic models used in the Nordic32 see [5].

Table A10: DISTR1 Mho settings used in the Nordic32, trip times are set to 2.5, 15 and 30 cycles for the three zones respectively.

Relay placement	Reach coverage	Branch No.	Zone 1 settings [pu]			Zone 2 settings [pu]			Zone 3 settings [pu]		
			Z magnitude	Angle	Radius of reach	Z magnitude	Angle	Radius of reach	Z magnitude	Angle	Radius of reach
4047	4043-4044-1044	1	0.016	84.289	0.008	0.018	84.289	0.009	0.046	86.765	0.023
4011	4021-4032-4044	1	0.012	86.186	0.006	0.068	84.289	0.034	0.111	81.113	0.055
4011	4022-4031-4041	1	0.040	84.289	0.020	0.048	84.289	0.024	0.088	84.031	0.044
4012	4022-4031-4042	1	0.028	83.480	0.011	0.043	83.630	0.021	0.115	83.059	0.057
4021	4032-4042-4044	1	0.032	84.289	0.016	0.048	82.875	0.010	0.082	74.610	0.041
4022	4031-4041-4061	1	0.032	84.28	0.016	0.048	83.817	0.024	0.089	82.827	0.044
4022	4031-4041-4062	2	0.032	84.289	0.016	0.048	83.817	0.024	0.089	82.827	0.044
4031	4032-4042-4045	1	0.008	84.289	0.004	0.020	83.722	0.010	0.064	83.404	0.032
4031	4041-4044-4051	1	0.032	81.469	0.016	0.046	81.835	0.023	0.074	82.760	0.037
4031	4041-4044-4051	2	0.032	81.469	0.016	0.046	81.835	0.023	0.074	82.761	0.037
4032	4042-4043-4046	1	0.032	75.937	0.016	0.044	76.403	0.022	0.058	77.919	0.029
4032	4044-4043-4046	1	0.040	83.157	0.020	0.052	83.201	0.026	0.062	83.376	0.031
4041	4044-4043-4046	1	0.024	84.289	0.012	0.032	84.289	0.016	0.042	84.289	0.021
4041	4061-4062-4063	1	0.009	82.405	0.004	0.049	82.558	0.024	0.071	83.093	0.035
4042	4044-4045-4062	1	0.016	84.289	0.008	0.024	84.289	0.056	0.056	83.682	0.028
4042	4043-4046-4047	1	0.012	82.402	0.006	0.016	82.626	0.008	0.028	83.480	0.014
4044	4032-4031-4041	1	0.040	83.157	0.020	0.070	83.480	0.035	0.152	83.493	0.076
1043	1041-1045-1042	1	0.048	80.537	0.024	0.085	81.202	0.042	0.246	81.703	0.121
1043	1041-1045-1042	2	0.049	80.538	0.024	0.085	0.085	0.042	0.246	81.703	0.121
1045	1041-1041-1043	1	0.097	82.875	0.048	0.133	82.661	0.066	0.198	82.152	0.099
1045	1041-1041-1043	2	0.097	82.875	0.048	0.133	82.661	0.066	0.198	82.152	0.099
1044	1043-1041-1045	1	0.064	82.875	0.032	0.093	82.568	0.046	0.199	81.984	0.099
1044	1043-1041-1045	2	0.064	82.875	0.032	0.093	82.569	0.046	0.199	81.985	0.099
1044	1042-1045-1041	1	0.226	82.271	0.113	0.343	81.964	0.172	0.611	81.432	0.305
1044	1042-1045-1041	2	0.226	82.271	0.113	0.343	81.964	0.171	0.611	81.432	0.305
1045	1042-1044-1043	1	0.243	80.537	0.121	0.361	80.809	0.180	0.602	81.413	0.301
1041	1043-1044-1042	1	0.049	80.537	0.024	0.077	81.027	0.038	0.198	81.984	0.099
1041	1043-1044-1042	2	0.048	80.537	0.024	0.077	81.027	0.038	0.198	81.984	0.099
1041	1045-1042-1044	1	0.097	82.875	0.048	0.181	82.093	0.091	0.481	81.328	0.024
1041	1045-1042-1044	2	0.097	82.875	0.048	0.182	82.093	0.091	0.4816	81.328	0.0241
1043	1044-1042-1045	1	0.064	82.875	0.032	0.137	82.626	0.068	0.424	82.137	0.212
1043	1044-1042-1045	2	0.064	82.875	0.032	0.137	82.626	0.068	0.424	82.137	0.212
1042	1044-1043-1041	1	0.226	82.271	0.113	0.299	82.303	0.149	0.375	82.345	0.188
1042	1044-1043-1041	2	0.226	82.271	0.113	0.299	82.304	0.149	0.375	82.345	0.188
1042	1045-1041-1043	1	0.243	80.538	0.122	0.328	80.710	0.164	0.437	81.184	0.219

B

System protection relay model data sheet

Table A1: Model CONs, STATEs, VARs and ICONs

CONs	Value	Description
G	$0.2 \cdot 2\pi$	TPSI filter time constant
G+1	5	AVR set points increase (%)
G+2	35	Load shed step (%)
G+3	1.8991	Generator bus 1012 rated field current pu.
G+4	1.8991	Generator bus 1013 rated field current pu.
G+5	1.8991	Generator bus 1014 rated field current pu.
G+6	1.8991	Generator bus 1021 rated field current pu.
G+7	3.0618	Generator bus 1022 rated field current pu.
G+8	3.0618	Generator bus 1042 rated field current pu.
G+9	1.8991	Generator bus 1043 rated field current pu.
G+10	1.8991	Generator bus 2032 rated field current pu.
G+11	1.8991	Generator bus 4011 rated field current pu.
G+12	1.8991	Generator bus 4012 rated field current pu.
G+13	1.8991	Generator bus 4021 rated field current pu.
G+14	2.9579	Generator bus 4031 rated field current pu.
G+15	3.0618	Generator bus 4041 rated field current pu.

CONs	Value	Description
G+16	3.0618	Generator bus 4042 rated field current pu.
G+17	3.0618	Generator bus 4047 rated field current pu.
G+18	3.0618	Generator 2 bus 4047 rated field current pu.
G+19	3.0618	Generator bus 4051 rated field current pu.
G+20	3.0618	Generator 2 bus 4051 rated field current pu.
G+21	3.0618	Generator bus 4062 rated field current pu.
G+22	3.0618	Generator bus 4063 rated field current pu.
G+23	3.0618	Generator 2 bus 4063 rated field current pu.
G+24	1.8991	Generator bus 4071 rated field current pu.
G+25	1.8991	Generator bus 4072 rated field current pu.

STATES	Value	Description
S		TPSI filter STATE

VARs	Value	Description
D		Filtered TPSI (Output channel)
D+1		Internal load shed timer
D+2		TPSI value (Output channel)
D+3		Internal voltage magnitude variable
D+4		Internal voltage angle variable
D+5		Lowest TPSI bus constant MVA load (Output channel)
D+6		Lowest TPSI bus constant admittance load (Output channel)
D+7		Lowest TPSI bus constant current load (Output channel)
D+8		Lowest TPSI bus number (Output channel)

ICONs	Value	Description
F	41	Bus index for VOLMAG function
F+1	42	Bus index for VOLMAG function
F+2	43	Bus index for VOLMAG function

ICONS	Value	Description
F+3	46	Bus index for VOLMAG function
F+4	47	Bus index for VOLMAG function
F+5	51	Bus index for VOLMAG function
F+6	61	Bus index for VOLMAG function
F+7	62	Bus index for VOLMAG function
F+8	63	Bus index for VOLMAG function
F+9	1011	Bus index for VOLMAG function
F+10	1012	Bus index for VOLMAG function
F+11	1013	Bus index for VOLMAG function
F+12	1014	Bus index for VOLMAG function
F+13	1021	Bus index for VOLMAG function
F+14	1022	Bus index for VOLMAG function
F+15	1041	Bus index for VOLMAG function
F+16	1042	Bus index for VOLMAG function
F+17	1043	Bus index for VOLMAG function
F+18	1044	Bus index for VOLMAG function
F+19	1045	Bus index for VOLMAG function
F+20	2031	Bus index for VOLMAG function
F+21	2032	Bus index for VOLMAG function
F+22	4011	Bus index for VOLMAG function
F+23	4012	Bus index for VOLMAG function
F+24	4021	Bus index for VOLMAG function
F+25	4022	Bus index for VOLMAG function
F+26	4031	Bus index for VOLMAG function
F+27	4032	Bus index for VOLMAG function
F+28	4041	Bus index for VOLMAG function
F+29	4042	Bus index for VOLMAG function
F+30	4043	Bus index for VOLMAG function
F+31	4044	Bus index for VOLMAG function
F+32	4045	Bus index for VOLMAG function

ICONS	Value	Description
F+33	4046	Bus index for VOLMAG function
F+34	4047	Bus index for VOLMAG function
F+35	4051	Bus index for VOLMAG function
F+36	4061	Bus index for VOLMAG function
F+37	4062	Bus index for VOLMAG function
F+38	4063	Bus index for VOLMAG function
F+39	4071	Bus index for VOLMAG function
F+40	4072	Bus index for VOLMAG function

Include SYSPROTMODEL.dll in simulation.

In .dyr file:

```
1, 'USRMSC', 'TPSIFOR', 512, 0, 41, 27, 1, 15, ICON(F)-ICON(F+40), CON(G)-
CON(G+25)/
```

The structure of how PSS/E call models in the .dyr file requires that all listed ICONs and CONs are included.

The models .dll file also need to be imported to PSS/E when running simulations. When using Python, this is achieved by using the command:

```
psspy.addmodellibrary(r"Z:\PATH\SYSTEMPROTECTIONMODEL.dll")
```

C

System protection relay model Fortran code

The code is written using Intel Visual Fortran 2005 with the format .F90 and is compiled using PSS/E 34 Environment manager with the following steps:

1. Intel Visual Fortran must be installed and linked to the Enviroment manager. Different versions of Intel Visual Fortran can have differences in syntax.
2. Choose output folder and name the model .dll file.
3. Add .F90 file as a "User Model Fortran Source File".
4. Compile using "Compile + Create DLL"
5. Check log for errors. Only syntax errors are shown here. Errors in model functions have to be troubleshooted through writing to the Output bar in PSS/E with the use of *WRITE (ITERM, *) 'EXAMPLE TEXT', EXAMPLE VARIABLE* in the model code.

The model is not generic and changes have to be made in the code for it to suit other systems. These changes are mainly to be made for the declaration of constants and variables. These changes include:

- The bus array "BUSNR" which shall include all buses in the system and the size should be the same as the number of buses. (Line 8 in the source code of the model)
- The generator bus array "GENBUSNR" shall include bus numbers of all generator buses in the system. (Line 10 in the source code of the model)

- The connection matrix "conn" needs to be changed so that it contains connections between all buses. (Lines 51-91 in the source code of the model)

The VOLMAG function used for measurements of voltage and angle requires bus number in the format ICON as input, The number of ICONs therefore need to be changed if the system is changed. The number of ICONs that the model uses is set in the .dyr file and shall be the same as the number of buses.

If the number of generator buses is changed the number of CONs that the model uses also have to be changed in the .dyr file. The number of CONs must be equal to the number of generators plus four.

The model only considers active power paths as this proved to be the critical part for the Nordic32. Reactive power paths were therefore not considered in order to decrease the simulation time. This might not be true for other systems, where the reactive power paths also need to be considered. The principle of finding reactive power paths is the same as for the active with the modification that bus voltages is considered instead of angles when finding paths [24]. An additional path finding loop will need to be added for finding the reactive paths. Note that this will almost double the time consumption of the model.

The model code in Fortran can be seen on the next page.


```

105     STATE(S) = VAR(D+2)
106     VAR(D+1)=1000
107     !VREFCHECK(9)=1
108     VREFCHECK(22)=1
109     VREFCHECK(23)=1
110 ENDIF           !End of Mode 1
111
112 IF (MODE.EQ.2) THEN ! Mode=2
113     DSTATE(S) = (VAR(D+2)-STATE(S))/CON(G)
114 ENDIF           !End of Mode 2
115
116 IF (MODE .EQ. 3) THEN           !Mode=3 Update output signal from model
117 DO Q=0,SIZE(BUSNR)-1,1           !Voltage magnitude and angle measurement
118     CALL VOLMAG(F+Q,D+3,D+4)
119     voltvector(Q+1)=VAR(D+3)
120     anglevector(Q+1)=VAR(D+4)
121 END DO
122
123 !TPSI-LOOP START
124     j=0
125     k=0
126     n=1
127     m=1
128     NONzeros=0
129     stopp=.true.
130
131     !Find Active power buses,(Buses which voltage angle is
132     !"ahead" of all other busses connected to that bus)
133     DO j=1,SIZE(BUSNR),1 !Loop through connection matrix to find sending buses
134         n=1
135         angledeg=0.0d0
136         DO k=1,SIZE(BUSNR),1
137             connpos=conn(j,k)
138             IF (connpos==1) THEN !Compare bus angle to connected bus(es) angle(s)
139                 angledeg(n)=anglevector(j)-anglevector(k)
140                 n=n+1
141             END IF
142         END DO
143         NONzeros=COUNT(angledeg/=0)
144         ALLOCATE(angle2(NONzeros))
145         angle2=PACK(angledeg,angledeg/=0)
146         IF(all(angle2>0))THEN
147             activepowerbuses(m)=j !Store sending bus in array of
148             m=m+1                 !sending buses for use in TPSI algorithm
149         END IF
150         DEALLOCATE(angle2)
151     END DO
152
153     NONzeros=COUNT(activepowerbuses/=0)
154     ALLOCATE(activepowerbuses2(NONzeros))
155     activepowerbuses2=PACK(activepowerbuses,activepowerbuses/=0)
156
157     !!!!!!!!!!!!!!!!!!!!!!!!!!!!!!!!!!!!!!!!!!!!!!!!!!!!!!!!!!!!!!!!!!!!!!!
158     !Initiation of TPSI algorithm
159     TPSI=0.6
160     number_of_paths=0
161     unstablepaths=0
162     stablepaths=0
163     ALLOCATE(stack2(1))
164     ALLOCATE(childs2(1))
165     DO APbuscounter=1,SIZE(activepowerbuses2),1
166     !Loop though all sending end buses
167     !Reset values for next sending end bus
168         j=0
169         k=0
170         n=1
171         m=1
172         NONzeros=0
173         stopp=.true.
174         back=.false.
175         startbus=activepowerbuses2(APbuscounter)
176         A=startbus
177         stackindex=1
178         visitedindex=2
179         visited=0.0d0

```

```

180     stack=0.0d0
181     visited(1)=A
182     stack(1)=A
183
184     !Path finding algorithm
185     DO WHILE (stopp==.true.)
186         IF ((back==.true.) .and. (ALL(stack==0))) THEN
187             stopp=.false.           !Exit if path is found
188             EXIT
189         END IF
190         !Reset connditions for path iteration
191         back=.false.
192         childs=0.0d0
193         j=0
194         k=0
195         n=1
196         m=1
197
198         DO k=1, SIZE(BUSNR), 1
199             childangle=anglevector(A)-anglevector(k)
200             connpos=conn(A, k)
201             IF (connpos==1 .and. childangle>0) THEN
202                 childs(n)=k           !Find conneced buses with increasing voltage angle
203                 n=n+1;
204             ELSE IF (ALL(childs==0) .and. (k==SIZE(BUSNR)) .and. (stackindex>1)) THEN
205                 DEALLOCATE(stack2)     !If end of path is found
206                 NONzeros=COUNT(stack/=0)
207                 ALLOCATE(stack2(NONzeros))
208                 stack2=PACK(stack, stack/=0)
209                 number_of_paths=number_of_paths+1
210                 TPSI_pathsum=0
211                 DO stackL=1, (SIZE(stack2)-1), 1 !Calculate the TPSI value of the path
212                     TPSI_pathsum=TPSI_pathsum+((voltvector(stack2(stackL))-voltvector(stack2
                                     (stackL+1)))*cosd(anglevector(stack2(stackL))-anglevector(stack2(stackL+1))))*cosd
                                     (anglevector(stack2(1))-anglevector(stack2(stackL))))
                                     ↙
                                     ↘
213                 END DO
214                 TPSI_new=(0.5*voltvector(stack2(1))-(TPSI_pathsum)
215                 IF ((TPSI_new<TPSI)) THEN !Save new TPSI value if lower than previous value
216                     TPSI=TPSI_new
217                     stablepaths=stablepaths+1
218                     TPSIBUS=stack(stackindex)
219                 END IF
220                 stack(stackindex)=0
221                 stackindex=stackindex-1
222                 A=stack(stackindex)
223                 back=.true.
224                 EXIT                               !Exit loop when new path is found
225             ELSE IF (ALL(childs==0) .and. (k==SIZE(BUSNR)) .and. (stackindex<=1)) THEN
226                 back=.true.
227                 stack(stackindex)=0 !Check if all paths have been found
228             END IF                               !for the current sending end bus
229         END DO
230
231     IF (back==.false.) THEN                       !Find next bus in path
232         DEALLOCATE(childs2)
233         childcheck=1
234         NONzeros=COUNT(childs/=0)
235         ALLOCATE(childs2(NONzeros))
236         childs2=PACK(childs, childs/=0)
237         DO y=1, SIZE(childs2), 1 !Loops to prevent the same path to be used twice
238             visitedL=SIZE(visited) !and to choose the next bus in the current path
239             DO k=1, visitedL, 1
240                 IF (visited(k)==childs2(y)) THEN
241                     visitedcheck=.true.
242                     EXIT
243                 ELSE IF (k==visitedL .and. visited(k)/=childs2(y)) THEN
244                     visitedcheck=.false.
245                 END IF
246             END DO
247         IF (visitedcheck==.false.) THEN !Continue with path if connected
248             A=childs2(y) !buses have not been visited though
249             stackindex=stackindex+1 !this bus for the current path
250             stack(stackindex)=A
251             visited(visitedindex)=A
252             visitedindex=visitedindex+1

```

```

253         childcheck=childcheck+1
254         EXIT
255     ELSE IF (childcheck==SIZE(chilids2)) THEN
256         stack(stackindex)=0 !If no conected buses, revert to previous bus
257         stackindex=stackindex-1
258         back=.true.
259         IF (stackindex>0) THEN
260             A=stack(stackindex)
261         END IF
262         DO p=1,SIZE(visited),1 !Remove buses connected to current bus from
263             DO j=1,SIZE(chilids2),1 !visited so that they can be visited once
264                 IF (visited(p)==chilids2(j)) THEN !again through another "parent" bus.
265                     visited(p)=0
266                 END IF
267             END DO
268         END DO
269     ELSE
270         childcheck=childcheck+1
271     END IF
272 END DO
273 END IF
274 IF ((back==.true.).and.(ALL(stack==0))) THEN
275     stopp=.false.
276     EXIT
277 END IF
278 END DO
279 END DO
280 !TPSI-LOOP FINISHED
281
282 DO y=1,SIZE(GENBUSNR),1
283     GENIDENTIFIER='1'
284     IF (GENBUSNR(y)==GENBUSNR(y-1)) THEN
285         GENIDENTIFIER='2'
286     END IF
287     IBUS=GENBUSNR(y)
288     CALL GENCHK (IBUS,GENIDENTIFIER,GENINDEX,'error')!Get machine index
289     GENINDEXARRAY(y)=GENINDEX !Machine index array
290     GENOEL(y)=VOEL(GENINDEX) !OEL activation array
291     GENVREF(y)=VREF(GENINDEX) !VREF array
292     GENFIELD(y)=XADIFD(GENINDEX) !Machine field current array
293 END DO
294
295 IF ((COUNT(GENOEL/=0))>0).AND.(CON(G+1)>0).AND.(STATE(S)<0.15)) THEN
296     DO y=1,SIZE(GENOEL),1 !Increase AVR set points when an OEL is activated and TPSI<0.
297         15
298         IF ((GENOEL(y)==0).AND.(GENVREF(y)<1.1).AND.(GENFIELD(y)<(CON(G+3+y)*1)).AND.
299             (VREFCHECK(y)==0)) THEN
300             VREF(GENINDEXARRAY(y))=GENVREF(y)*((CON(G+1)/100)+1) !AVR set point increase
301             VREFCHECK(y)=1 !Set check so the current
302             WRITE ( ITERM, * ) !generator will not increase AVR set point again
303             WRITE ( ITERM, * ) 'NORDIC32 SYSTEM PROTECTION RELAY MODEL'
304             WRITE ( ITERM, * ) 'VREF INCREASE AT BUS' , GENBUSNR(y), 'by', CON(G+1), '%'
305             WRITE ( ITERM, * )
306         END IF
307     END DO
308 END IF
309
310 IBUS=BUSNR(TPSIBUS)
311 CALL LODCHK (IBUS, '1', I)!Get lowest TPSI load index
312 VAR(D+5)=CLODFR(1,I) !Constant MVA
313 VAR(D+6)=CLODFR(2,I) !Constant admittance
314 VAR(D+7)=CLODFR(3,I) !Constant current
315 VAR(D+8)=BUSNR(TPSIBUS) !Lowst TPSI bus number to output variable
316 VAR(D+1)=VAR(D+1)+1 !Load shed delay timer increase
317
318 IF ((STATE(S)<CON(G+3)).AND.(VAR(D+1)>1000).AND.(CON(G+2)>0)) THEN
319     CLODFR(1,I)=VAR(D+5)*(1-(CON(G+2)/100)) !Shed constant MVA
320     CLODFR(2,I)=VAR(D+6)*(1-(CON(G+2)/100)) !Shed constant admittance
321     CLODFR(3,I)=VAR(D+7)*(1-(CON(G+2)/100)) !Shed constant current
322     VAR(D+1)=0 !Reset timer
323     WRITE ( ITERM, * )
324     WRITE ( ITERM, * )
325     WRITE ( ITERM, * ) 'NORDIC32 SYSTEM PROTECTION RELAY MODEL'

```

```
326     WRITE ( ITERM, * ) 'LOAD SHEDDED AT BUS:',IBUS,' BY ', CON(G+2)
327     WRITE ( ITERM, * )
328     WRITE ( ITERM, * )
329     END IF
330 7 VAR(D+2) = TPSI
331     VAR(D)=STATE(S)
332     ENDIF           !End of Mode 3
333
334     IF (MODE .EQ. 4) THEN !Mode 4 Update variable NINTEG
335         NINTEG = MAX(NINTEG,S)
336         RETURN
337     ENDIF           !End of Mode 4
338
339     IF (MODE .EQ. 8) THEN !Mode 8 Parameter description for ADD/EDIT constants
340         CON_DSCRPT(1)='Title of CON1'
341         CON_DSCRPT(2)='Title of CON2'
342     ENDIF           !End of Mode 8
343     ENDIF
344 END SUBROUTINE TPSIFOR
```